RIGA TECHNICAL UNIVERSITY
Faculty of Computer Science and Information Technology
Institute of Computer Control, Automation and Computer Engineering

Kamran Ayub
Doctoral Student of the Study Program "Automation and Computer Engineering"

RESEARCH ON IMPULSE RADIO'S FEASIBILITY FOR WIRELESS SENSOR NETWORK AND DEVELOPMENT OF NEW COMPATIBLE ARCHITECTURE

Summary of the Doctoral Thesis

Scientific Supervisor
Dr.habil.sc.comp., Professor
V. ZAGURSKIS

RTU Press
Riga 2016

Ayub K. Research on Impulse Radio's Feasibility for Wireless Sensor Network and Development of New Compatible Architecture. Summary of the Doctoral Thesis. – R.: RTU Press, 2016. – 48 p.

Printed according to the Resolution of the Institute of Computer Control, Automation and Computer Engineering, as of 25 May 2016, Minutes No.12200-2/3.

ISBN 978-9934-10-882-2

DOCTORAL THESIS

PROPOSED TO RIGA TECHNICAL UNIVERSITY FOR THE PROMOTION TO THE SCIENTIFIC DEGREE OF A DOCTOR OF ENGINEERING SCIENCES (*Dr.sc.ing.*)

To be granted the scientific degree of Doctor of Engineering Sciences, the present Doctoral Thesis has been submitted for the defence at the open meeting of RTU Promotion Council on December 21, at the Faculty of Computer Science and Information Technology, 1 Setas Street, Room 202.

OFFICIAL REVIEWERS

Professor *Dr. habil. sc. ing.* Leonids Novickis
Riga Technical University, Latvia

Professor *Dr. sc. ing.* Aleksandrs Grakovskis
Transport and Telecommunication Institute, Latvia

Professor *Dr.* Husrev Taha Sencar
TOBB University Ankara, Turkey

DECLARATION OF ACADEMIC INTEGRITY

I hereby declare that the Doctoral Thesis submitted for the review to Riga Technical University for the promotion to the scientific degree of Doctor of Engineering Sciences is my own and does not contain any unacknowledged material from any source. I confirm that this Thesis has not been submitted to any other university for the promotion to other scientific degree.

Kamran Ayub …………………………….(Signature)

Date: ………………………

The Doctoral thesis has been written in English. It consists of introduction, 5 chapters, conclusions, bibliography with 121 reference sources, and an appendices. It has been illustrated by 76 figures. The volume of the present Doctoral Thesis is 149 pages.

TABLE OF CONTENTS

Abbreviations

ADC	Analog to Digital Converter
BAN	Body Area Network
BER	Bit Error Rate
BPAM	Binary Pulse Amplitude Modulation
BS	Base Station
CDMA	Code Division Multiple Access
CH	Cluster Head
CM	Channel Model
CSI	Channel State Information
DH	Delay-Hopped
DSP	Digital Signal Processing
E_b/N_o	Energy per bit to Noise power spectral density
FCFS	First Come First Serve
IPI	inter pulse interference
IR	Impulse Radio
ISI	Inter-Symbol Interference
LNA	Low Noise Aplifier
MAC	Medium Access Control (Layer)
MSI	Maximum Selection Interpolation
PA-MAC	Pilot-Assisted MAC
PAT	Pilot-assisted Transmission
PHY	Physical (Layer)
Pmax	Maximum Power
PPAM	Pulse Position Amplitude Modulation
QoS	Quality of Service
RF	Radio Frequency
Rx	Receiver
SNR	Signal to Noise Ratio
TH	Time Hopping
Tr	Resolution time of Receiver
TR	Transmitted Reference
TRDH	Transmitted Reference Delay-Hopped
Tx	Transmitter
U-MAC	Ultra Wideband MAC
UWB	Ultra-Wide Band
WBAN	Wireless Body Area Network
WSN	Wireless Sensor Network

INTRODUCTION

The primary aim of this research is to design a flexible UWB and WSN integrated architecture, which could be used effectively in all kind of WSNs. From the recent study, it was observed that most of the advanced issues with the Wireless Sensor Network are related to Physical and Radio layers. The MAC's compatibility with the physical layer and low duty cycle scheduling are the essentials for a WSN. These concerns are used as starting point of the research.

Theme Relevance

The Doctoral Thesis has not only thoroughly investigated the root causes but designed a flexible framework, which can be employed in both small and dense network. Thesis is mainly focused on two areas, MAC architecture, and PHY layer design.

The Doctoral Thesis uses Agile [1] approach where all the main identified issues are divided in sprints, and each sprint is resolved separately. On the resolution of individual sprints. All issues are jointly retested. At the end of research architecture is used on a hardware platform under a WBAN project "SMART Incubator". This over five-year long research has proved that the UWB is the most practical solution for wireless sensor network if it is used under the parameters of our given framework.

The Aim and Tasks

The aim of the Doctoral Thesis is to develop a compatible impulse radio based transmission architecture for wireless sensor network, which has self-organization capability.

The tasks are as follows:

1. To study and identify the communication bottlenecks of core layers of WSN Communication. *e.g., PHY, MAC.*
2. Targeting the issues from Task1, design a MAC algorithm which works in both conditions (low and heavy medium access requests)
3. To develop a radio architecture by evaluating the existing schemes, which is compatible with the MAC design and reliably works for WSN.
4. To design an effective, and reliable Clustering strategy for dense network environment.
5. To test the performance of proposed architecture to measure the self-organization, Energy saving, Consistency capabilities.
6. Implementation of architecture in a real life scenario.

Research Subject and Object

The research subject is Impulse Radio based wireless sensor network.
The objects are research on impulse radio's feasibility for wireless sensor network and development of new compatible architecture.

Thesis Statements to Be Defended

1. Impulse Radio is an effective Physical layer scheme for Wireless Sensor Network.

2. Transmitted Reference Delay Hoped Radio architecture is better Radio architecture than RAKE and WUR for Wireless Sensor Network.

3. The cross-layer relation between MAC and PHY improves Network lifetime.

4. Dynamic Clustering (based on COST function) approach is better than conventional clustering in WSN.

5. Following the designed framework, wireless sensor networks under Impulse Radio platform is practically applicable.

Scientific Methods Used

Analytical Survey: Of Wireless Sensor Network and Ultra-wideband.
Case Studies: of different existing medium access and radio solutions.
Logical reasoning: For every single adoption feature, that has helped to elaborate the proposed ideas.
Theoretical Analysis: By modeling the LLD (Low-level Design) and HLD (High-Level Design).
Qualitative & Statistical Analysis: By comparing our results with existing solutions. (TRDH Vs. RAKE, PA-MAC Vs. Leach etc.)
Hardware testbed : By using MAS-WBAN Testbed

Scientific Novelty

Scientific novelty of the Doctoral Thesis:

1. Problems of wireless sensor network under Impulse Radio is defined, based on the identified issues a framework is developed with following key points;

2. A multiphase MAC algorithm developed, which is compatible with WSN and has outclassed performance under IR-UWB physical layer;

3. A lightweight Radio Architecture (TRDH) developed which has capability of multiuser support and saves energy by avoiding the Channel state information;

4. Dynamic transmission range based Clustering adoption features added in the framework which enables the framework to work in both limited and dense network environment, also, provide Self-Organization capability;

Practical Application of Research Results

This research was conducted using a systematic approach. The developed Pilot assisted Medium access control (MAC) algorithm with Impulse radio ultra-wideband (IR-UWB) at PHY layer provides reliable, consistent, and energy efficient platform for WSN. It has flexibility to be used in the event based WSN, or in those networks where network traffic is not fixed and varies time to time. The multi-phase capability to handle network traffic makes the framework suitable to a vast variety of WSN, typically short-range wireless sensor networks where event based activities are noticed. Transmission under framework gives an excellent throughput, for example by comparing PA-MAC with U-MAC for "Average Throughput" and Average Delay. Performance of PA-MAC is far better than U-MAC. See Table 1.

Table 1. U-MAC vs. PA-MAC performance

Algorithm	**Avg. Throughput**	**No. of nodes**	**Avg. Packet Delay**
U-MAC	320 kbps	25	11 ms
PA-MAC	450 kbps	25	8.5 ms

Based on its reliability and excellent throughput, the framework could be adopted for time critical data networks, especially Body area Networks (BAN) and Personal Area Network (PAN). Military and Medicals are the major areas of interests. A unique integrated Radio architecture is used in the framework development, which is different from the existing solutions. The integrated radio architecture does not require channel estimation hence saves a massive amount of energy that makes it an ideal solution for continues monitoring sensor networks. A very common use of such network is road traffic congestion monitoring.

Beside proposed integrated Transmitted Reference and Delay hoped Radio architecture framework has very simple receiver circuitry and strong ability to avoid interferences from other medias [2], [3], [4] (e.g., Narrow band). That makes it a perfect choice for industrial applications where mixed Medias are used. Due to its simple Radio circuitry, the overall node price could be brought down. Subsidiary benefits as high network constancy, which could reduce operational expenses hence economic advantage could be achieved.

At the end of the research author has implemented it for a medical project SMART Incubator, where it was used on two different networks, fixed nodes and body attach nodes. The results were compared with simulation results, and it was noticed that framework works very well under short range time critical medical applications.

Scientific publications

1. Kamran Ayub, Zagurskis, V. SMART Incubator: Implementation of Impulse Radio-Ultra Wide Band Based PA-MAC Architecture in Wireless Body Area Network. 2nd International Conference IEEE, on Systems Informatics, Modelling and Simulation (SIMS-2016). Riga Technical University, Riga Latvia. June 2016 (*Paper accepted*)
2. Kamran Ayub, Zagurskis, V. Adoption features and approach for UWB Wireless Sensors Network based on Pilot Signal assisted MAC. International Journal of Communication Networks and Information Security (IJCNIS), Vol. 8, No 1 (2016), pp.40-46. ISSN: 2076-0930, Scopus & INSPEC indexed.
3. Kamran Ayub, Zagurskis, V. Performance evaluation of Self-Organizing feature of Cluster-based WSN for Pilot Assisted-MAC under IR-UWB. ICMSE – 2015 International Conference on Management Science and Engineering (22nd). IEEE Technology and Engineering Management Society. *Ieee-Xplore (Scopus Indexed).* ISBN: 978-14673-6511-6 *(Note: This paper has been submitted for indexing on IEEE-Xplore, EI, and Scopus and will be available soon)*
4. Kamran Ayub, Zagurskis, V. Technology Implications of UWB on Wireless Sensor Network-A detailed Survey. International Journal of Communication Networks and

Information Security (IJCNIS). Vol. 7, No. 3, 2015. ISSN: 2076-0930. *Scopus & INSPEC Indexed*. ISSN: 2076-0930

5. Kamran Ayub, Zagurskis, V. IR-UWB Radio Architecture for Wireless Sensors Network based on Pilot Signal Assisted MAC. International conference IEEE, NTMS-2014, Sixth International Conference on New Technologies, Mobility and Security. pp.1–5. ISBN 978-1-4799-3223-8 *Ieee-Xplore (Scopus)*.
6. Kamran Ayub, Zagurskis, V. Pilot Signal Assisted Ultra-Wideband Medium Access Control Algorithm for Wireless Sensor Networks. Telecommunications Forum (TELFOR) 21st.2013,pp.184-187, ISBN 978-1-4799-1420-3. *Ieee-Xplore (Scopus Indexed).*

Scientific conferences

1. 2nd International Conference IEEE, on Systems Informatics, Modelling and Simulation (SIMS-2016). Riga Technical University, Riga Latvia. June 2016 (*Paper accepted*).
2. International conference IEEE 21st Telecommunications Forum (TELFOR)-2013, November, 26-28 TELFOR 2013, Telecommunications Society, School of Electrical Engineering, University of Belgrade, IEEE Communications Society. The Sava Centre Belgrade, Serbia.
3. International conference IEEE, NTMS-2014, Sixth International Conference on New Technologies, Mobility and Security. IEEE Communications Society, IFIP, ADCO, March 30th to April 2nd, 2014, Zayed University Dubai UAE.
4. ICNGCCT 2015 – 2nd International Conference on Next Generation Computing and Communication Technologies, Zelus, MTS, CZRICA, Eye of Riyadh. 22-23 April -2015. Dubai, United Arab Emirates (UAE).
5. International conference IEEE, ICMSE – 2015 International Conference on Management Science and Engineering (22nd). IEEE Technology and Engineering Management Society, 19-22 October -2015. Dubai, United Arab Emirates (UAE)

Structure of the Doctoral Thesis

The Doctoral Thesis consists of five chapters. The first chapter gives a brief overview of Medium Access Control layer, underneath algorithm architecture. The second chapter is based on the Radio Layer, its architecture design and its compatibility with MAC layer, for better understanding its performance is compared with RAKE and Wake-up architectures.

After MAC and PHY layer design third chapter is focused on the topology, here multiple adaption features are added specifically a new dynamic Clustering technique. Chapter thoroughly evaluates the performance of adaption features. The fourth chapter assesses the Self-Organization capability of the framework. Multiple scenarios were designed to check the self-healing capability of the framework from all perspectives.

The last chapter covers the practical implementation of the architecture on WBAN platform under a project called “SMART Incubator”. Outcomes of hardware implementations are further compared with the simulation results. That gives a clear picture of PA-MAC framework’s flexibility, its measurements, and performance in a real scenario.

1. PILOT SIGNAL ASSISTED MAC ALGORITHM

To avoid heavy channel estimation, the author has used Impulse Radio (UWB) with PAT technique that improves synchronizations and reduces the probability of collision. The pilot signal is used as a reference signal, which provides control and supervision for wireless communication. To create a strong synchronization structure, Pilot signal is an excellent choice for UWB. Figure 1.1 shows power spectral density of a UWB- doublet (pilot and payload). Proposed MAC algorithm works around the Pilot signal which is used with impulse radio (UWB).

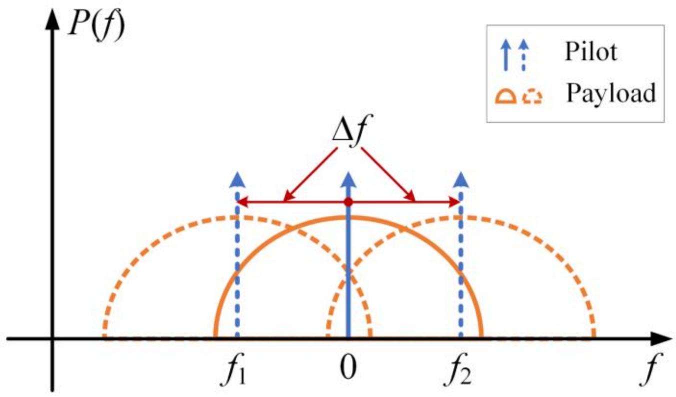

Fig. 1.1. Power spectral density of the pilot and payload [5]

Pilot signal works under IR-UWB Doublet where the 1st pulse is Pilot and 2nd works as payload Figure 1.1. The underneath MAC Algorithm uses multi-phase scheduling strategy Figure 1.3, and saves energy by eliminating channel estimation. MAC operations in the algorithm are divided into two phases. The first phase is used for the low access request and works on FCFS (first come first serve) basis. Once Channel requests increase to the level where the collision occurs, algorithm triggers to the phase 2. Synchronization and scheduling are planned in a proper manner before access to media is granted. Each node gets access as per the payload size. During phase 2; at the end of each round, priority is recalculated, and if there are no media access requests, algorithm triggers back to phase1.

To gain multi-access capability and to distinguish between delayed signal, DH (delay-hopped) code is used Figure 2.1. Use of DH codes with Transmitted Reference improves the throughput [6], [7] and provides multi users accessibility.

1.1 Proposed Algorithm

Assumptions: Signal duration is assumed more than *Tr* (Resolution Time of the receiver). Time (duration) is proportional to the priority ($T \propto Pr$). A simple network topology is selected, and a single hop, single cluster, with all member nodes have different priorities is used. It was assumed that there is no hidden or expose node problem. Round Robin priority algorithm [8] with minor modifications is used. Following are the core modifications added in the RR-Algorithm.

1- Each node will get only one access slot in each round, means after Tx and Rx node will go to the sleep mode and will not be considered again for that round polling.

2- At the end of each round, CH will design a new schedule with the help of pilot signal. Only nodes in the active state will be selected for the scheduling. If any node becomes active after schedule has been defined, it will wait for the next priority schedule.

3- High priority will be given to the nodes have not completed their Tx turn in the previous round.

4- If the time of arrival of two nodes is same, priority will be decided based on "shortest job first".

5- If CH does not get any media access request, the algorithm will transfer the control to phase1.

Algorithm

The core points of algorithm codes are given below.

Initialization	Initially all active nodes will set their priority timer Tp = Tmax (Maximum allowed time for a node) Tmax = Ntr + Tpac + 3tr *// where, N= number of Nodes, tr= Receivers' resolution time,* *//Tpac= Size of data frame, Tp= Priority Time} Input N, Tr, etc.*
(Phase1) Step1	

	//FCFS- No priority scheduling- best for low activity
	for(i = 1 to N) *//All nodes will set Tp to Tmax*
	Tp(n(i))=Tmax;
	While(Tp≠0) *//During Priority time*
	Node State= Rx *// { Listen while Tp }*

Step2	*//After Tp (Priority Time)* Node State = Tx(Pilot) *// If interested for Tx* If Media≠ IDLE *//If media is not idle -Collision* Go to Phase 2 *//Synchronize and Prioritize the communication* Else *//Continue till collision* Node State= Tx(data) i++ ; *// Next node*
(Phase2)	Synchronization and Priority scheduling *//Tp will be used for Tx*

Step 3	*Synchronize ( ); // Function call to synchronize
	*Prioritize ( ); // Function call to set Priority
	*TR-DH UWB- will synchronize, Round Robin will be used for Priority scheduling

Step 4	If Return(of above)= NULL or Active n =0 *// No active node or all nodes has* completed the tx GoTo Phase 1 : *// due to low activity go-to phase 1* Else go-to Step 5 :

Step 5	For(j= 1 to N) *// for all active nodes* Calculate Tp[j]; *// priority time* While Tp(j)≠0 *// during the priority time* Tx Pilot >> Tx Data; *// Tx Pilot followed by Tx (data)*
Step 6	switch (Tx & Tp) *// conditional Control* <u>case 1</u> : Tx =complete & Tp=*0* *// If Transmission completes, as per schedule* Node state =Rx( ) *// Rx( ) is a thread, will keep the* *//node in Rx state and control to the next node.* Break; *// Next node* <u>case 2</u> : Tx=complete & Tp ≠0 *// If Transmission //complete but Still Priority Time* Node state=Rx( ) *//Rx( ) is a thread, will keep the node in Rx state* Break; *// Stop Transmitter and control to Next node* <u>case 3</u> : Tx≠ complete & Tp=0 Node state = Tx *// Continue Tx (vulnerable time)* If collision: Node State = Rx( ) break; *// stop Tx and control to next node* Else Node State= Rx( ) *// Rx( ) is a thread* Break; Thread Rx( );{ for k=0; k< Tp ;k++) }if node=Idle Node State = Sleep else Node State= Rx; Rx( ) ; *// Each node will listen (Rx) same amount as Tx and will go to Sleep after that.*

1.2 Time Diagrams

For the better understanding of algorithm behavior, worst case scenarios were created and tested. Here T_X = Transmit, T_P = Priority, R_X = Receive, SL = Sleep, P = Pilot, and A = Active. Let's assume, 3 nodes n1, n2, n3 are active nodes and have some amount of data to transmit.

1st Round: Initially all nodes set Tp = Tmax, and their priorities are n3 = 1, n1 = 2, n2 = 3. All will Listen (Rx) during Tp and will send Pilot signal followed by data for transmission. Initially, all are assumed in the sequence, and no collision is detected Figure 1.2(a).

Nodes	TP	0	1	2	3	4	5	6	7	8	9	10	11	12	13	14	15	16	17	18	19	20	21	22	23	24	25	26	27	28
n1	=2	A	Tp							P	TX	TX	TX	SL	RX	RX	RX	RX	P	TX	TX	TX	RX	RX	RX	RX	RX	RX	RX	RX
n2	=3	A	Tp											P	TX	TX	TX	TX	SL	RX	RX	RX	RX	RX	RX	P	TX	TX	TX	TX
n3	=1	A	Tp				P	TX	TX	SL	RX	RX	RX	RX	RX	RX	RX	RX	RX	RX	RX	RX	P	TX	TX	RX	RX	RX	RX	RX
n4	=4																												A	P
n5	=5																												A	P

Fig. 1.2(a). Nodes in phase 1.

2nd Round: At 27, two new nodes n4, n5 activated, and send Pilot signals for media access, which got collided with existing n2's Tx. At this stage Phase, 2 will be activated.

2nd Round (Ideal Case): Nodes are Tx-ing during Tp and listens (Rx) for the same amount of time (as Tp) after that they go to Sleep (remains in the Sleep mode, until having another request for Tx). All nodes get activated at the scheduled time; in this round node, n3 is not active as it has nothing to send, so time slot was not allocated to n3. Figure 1.2(b).

	32	33	34	35	36	37	38	39	40	41	42	43	44	45	46	47	48	49	50	51	52	53	54
Pin= Tp=4	SL	SL	SL	SL	SL	SL	SL	SL	SL	SL	SL	SL	SL	SL	P	TX	TX	TX	TX	RX	RX	RX	RX
Pin=Tp=1	P	TX	TX	TX	RX	RX	RX	SL	SL	SL	SL	SL	SL	SL	SL	SL	SL	SL	SL	SL	SL	SL	A
Sleep	SL	SL	SL	SL	SL	SL	SL	SL	SL	SL	SL	SL	SL	SL	SL	SL	SL	SL	SL	SL	SL	SL	A
Pin=Tp=2	SL	SL	SL	SL	P	TX	TX	TX	TX	RX	RX	RX	RX	SL	SL	SL	SL	SL	SL	SL	SL	SL	A
Pin=Tp=3	SL	SL	SL	SL	SL	SL	SL	SL	SL	P	TX	TX	TX	TX	RX	RX	RX	RX	SL	SL	SL	SL	A

Fig. 1.2(b). Nodes in phase 2-Ideal case.

2

2nd Round (Tx outside the Tp)-unsuccessful: By assuming that Nodes are Tx-ing during Tp and then go to Sleep. Here node n3 could not complete Tx within its Tp, and transmission remains continue in the vulnerable window because it’s n2's turn (n3’s tx will be blocked). Figure 1.2(c).

	58	59	60	61	62	63	64	65	66	67	68	69	70	71	72	73	74	75	76	77	78
Pin=Tp=1		P	TX	TX	RX	RX	SL	SL	SL	SL	SL	SL	SL	SL	SL	SL	SL	SL	SL	SL	SL
Pin=Tp=3		SL	SL	SL	SL	SL	SL	SL	SL	SL	SL	P	TX	TX	RX	RX	SL	SL	SL	SL	SL
Pin=Tp=2		SL	SL	SL	SL	P	TX	TX	TX	TX	TX	TX	RX	RX	RX	RX	RX	SL	SL	SL	SL
Pin=Tp=5		SL	SL	SL	SL	SL	SL	SL	SL	SL	SL	SL	SL	SL	SL	SL	P	TX	RX	SL	SL
Pin=Tp=4		SL	SL	SL	SL	SL	SL	SL	SL	SL	SL	SL	SL	SL	P	TX	RX	SL	SL	SL	SL

Fig. 1.2(c). Nodes in phase 2- Tx outside.

***2nd Round (Tx outside the Tp window)-Successful**:* By supposing that n4 could not complete its Tx within Tp, and it continues Tx in the vulnerable window, as there is no other node scheduled for that time, it successfully completes its transmission (Tx) Figure 1.2(d).

	58	59	60	61	62	63	64	65	66	67	68	69	70	71	72	73	74	75	76	77	78
Pin=Tp=1		P	TX	TX	RX	RX	SL	SL	SL	SL	SL	SL	SL	SL	SL	SL	SL	SL	SL	SL	SL
Pin=Tp=3		SL	SL	SL	SL	SL	SL	SL	SL	SL	SL	P	TX	TX	RX	RX	SL	SL	SL	SL	SL
Pin=Tp=2		SL	SL	SL	SL	P	TX	TX	TX	TX	TX	TX	RX	RX	RX	RX	RX	SL	SL	SL	SL
Pin=Tp=5		SL	SL	SL	SL	SL	SL	SL	SL	SL	SL	SL	SL	SL	SL	SL	P	TX	tx	tx	Rx
Pin=Tp=4		SL	SL	SL	SL	SL	SL	SL	SL	SL	SL	SL	SL	SL	P	TX	RX	SL	SL	SL	SL

Fig. 1.2(d). Nodes in phase 2-Collision.

1.3 Performance Analysis

Performance is tested by executing worst case scenarios. Mixim (Omnet++) based simulation platform is used for this purpose. Performance is compared with two close competitor’s “LEACH and U-Mac” Algorithms [9], [10].

For traffic generation, the author has set max and min time for generating a hello message (10 sec & 1 sec) respectively, beside that MSI Threshold is set to 15 %, and interference threshold = 50 % Both Tx power and Tx rate are adjusted as per 802.15.4a conditions. P_{max} (Maximum power) is kept 15 dBm. In the simulation 25 nodes are used (n = 25). As the scope of work is to analyze the performance of MAC-Algorithm, only MAC related parameters were adjusted. The traffic rate λ = (0.25 to 5.00) call/s. Table 1.1 summarizes the main simulation values.

Table 1.1. Simulation constraints

Parameter	Values	Parameter	Values
N (No of nodes)	5–25	*R* (bit rate)	850 kbps
P (Transmission power)	–15 dBm (39 μW)	*Tf* (pulse repetition time)	Modified able
Traffic rate (Poisson) λ	0.5–5.0 calls/s	η (background noise + interference)	$2.5 \times \mathbf{10^{-17}}$ mW/Hz
Payload size	160 bytes	γ (threshold)	5 dB
Simulation area(los)	25 × 25	α (path loss exp)	2.5

The performance is compared for throughput, Packet delay, and power consumption.

1.4 Flow Chart

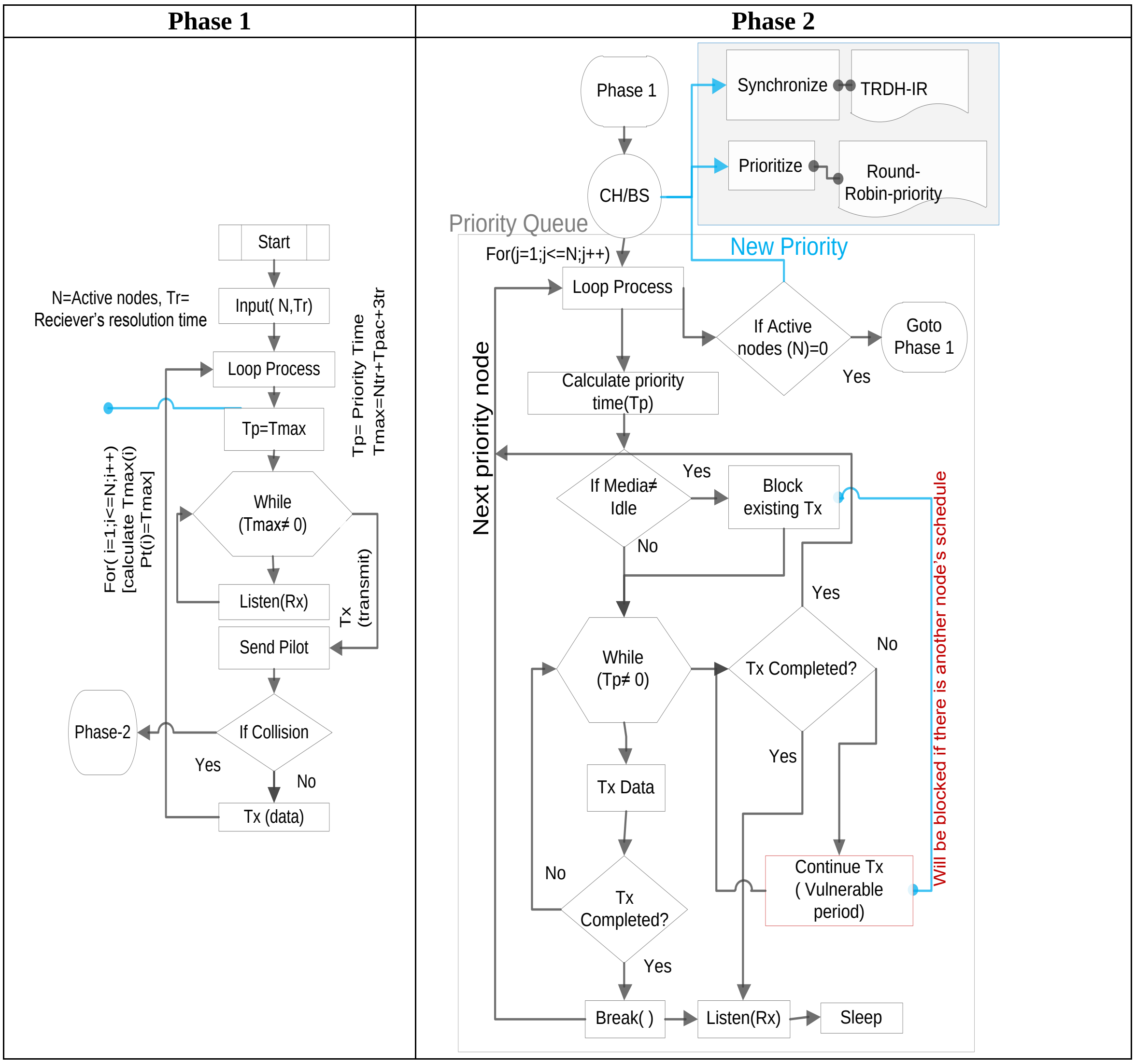

Fig. 1.3. Phase 1 (FCFS) and Phase 2 (Prioritized communication) of PA-MAC.

1.5 Simulation Results and Summary

Throughput Analysis

Figure 1.4(a) shows the overall achievable throughput of three algorithms. The throughput is based on single hop topology for all three algorithms. Average throughput of PA-MAC algorithm is about 500 kbps for 25 active nodes.

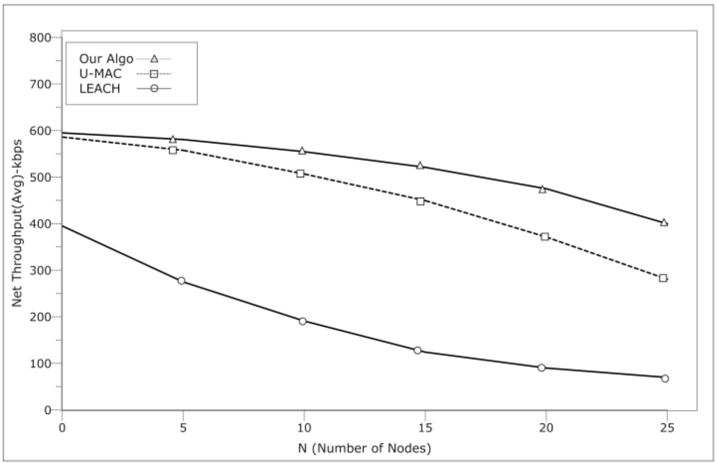

Fig. 1.4(a). Network Throughput (Average) v Number of Active Nodes

Although Throughput gradually decreases on some points but still the overall throughput is better than LEACH and U-MAC. It can be seen that as the number of nodes increases, both UWB based MACs beat the traditional LEACH this is because of admission control. The performance of LEACH quickly drops as the number of interference sources increase; this is due to the incompatibility of LEACH with UWB (radio) layer.

Average power consumption:

For the average power calculation chip-level energy-model described in [11] is used. Comparison of all three protocols is showed in Figure 1.4(b). It can be seen that proposed algorithm and U-MAC has almost the same energy consumption at startup, but with the increase of access requests (gradual increase of active nodes) more power is consumed, this is due to the waiting time for the schedule slot. At the peak (when n = 25) both U-MAC and LEACH are severely affected but our algorithm due to concrete scheduling and synchronization remains stable. The energy consumption of proposed algorithm remains under 0.2 mW throughout simulation (from n = 5 to 25) Figure 1.4(b). That shows the significant success of algorithm structure.

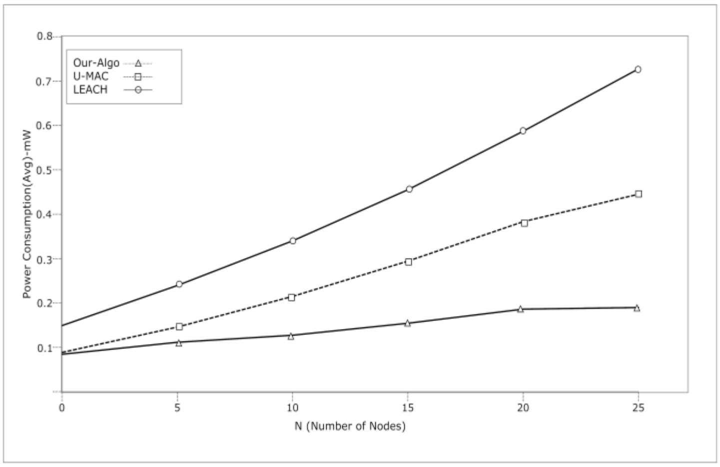

Fig. 1.4(b).Power consumption (Average.) vs. N.

Average Packet Delay:

The mean packet delay is an end-end delay of a packet from source to destination. Results for the packet latency are shown in Figure 1.4(c). The y-axis shows the average packet delay, whereas the x-axis is the number of nodes (N). As we can see that the average delay in case of our Algorithm is set at 5 milliseconds at the start (when 5 nodes are active), and does not cross to 0 ms even in a busy situation. That shows that proposed algorithm experiences the lowest delay compared to other algorithms. U-MAC has good packet delay too, but LEACH is severely affected by concurrent requests.

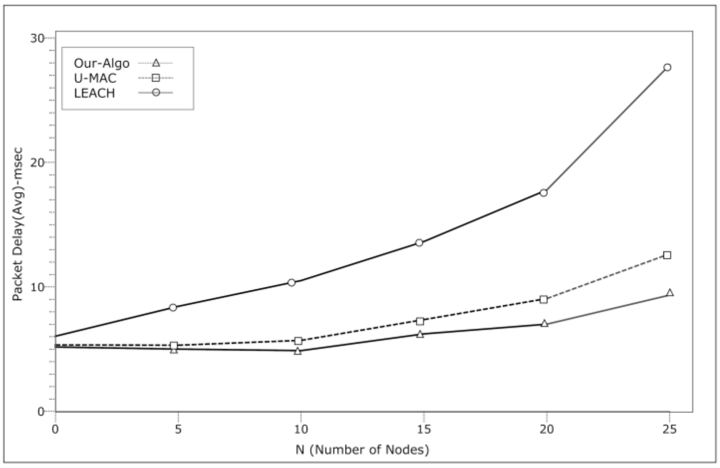

Fig. 1.4(c). Packet Delay vs. *N*(active nodes).

2. Radio Architecture Design for Pilot Signal Assisted MAC

In a traditional IR-UWB systems signal reception process receiver works through an analog correlator, which requires long synchronization time, complex assembly and channel estimation. On the other hand, Transmitted Reference structure is an attractive alternative. By simple integration of a DH code sequence, it can sidestep dense channel estimation, reduces the plea of synchronization accuracy, and can accumulate multipath energy; as a result, it is the best candidate for UWB based MAC.

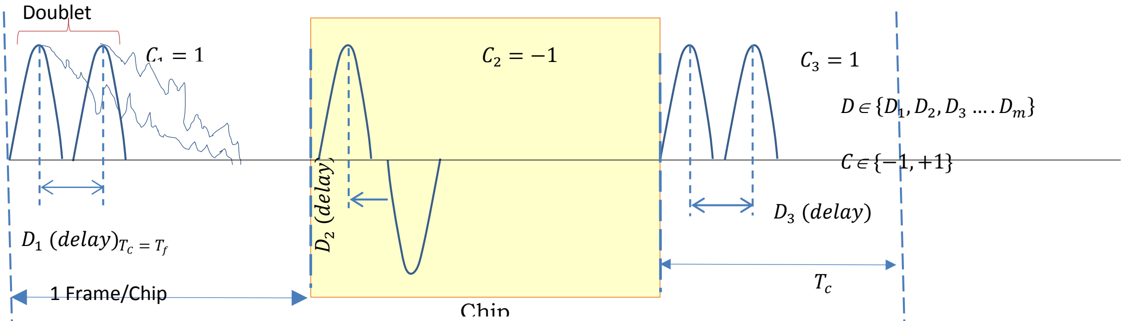

Pulses are transmitted as doublets, separated by delay D, C (Chip) has a Duration Tc and value could be +1/-1

Fig. 2.1. Impulse Radio UWB- TRDH pulse structure.

In Transmitted Reference structure, an impulse radio pulse pair (doublet) is used instead of single UWB pulse Figure 2.1. The first pulse works as a pilot and does not carry any information. It is delayed at the receiver to act as correlation pilot (reference) for the second pulse. In fact the data/information is carried in the 2nd pulse of the doublet. However the use of delay for TR communication is very limited to a few choices; I modified the architecture by adding DH-code of 2nd order Volterra model [12]. By relating a "Volterra sequence" it provides multi-access support.

2.1 Transmitted Reference with DH-Code (Volterra Model)

For TR-DH impulse radio, the transmitter is based on energy efficient pulse generator Figure 2.2, similarly, receiver design is modified to support Voltera scheme. Figure 2.3. Transceiver supports data rate from 5 kbps to 1.2 Gbps, and it can reach *BER* of about 2×10^{-4} for a link space of 10 m. By adjusting the data-rate the link distance and the *BER* can be estimated. The transmitter consumes as little as 600 μW of power, which makes it a good choice for short range WSN-applications. To evaluate the performance of Radio layer, *BER*/*SNR* is calculated here. Following are the key parameters used in the calculation.

$\omega(t)$ = pulse waveform.

N_p = Transmitted Pulses

$d_k \in \{0;\ 1\} \rightarrow$ symbols for BPPM

$a_k \in \{-1;\ 1\}$ $\rightarrow$ symbols for BPAM

$D \geq T_\mathrm{p} + T_g$ $\rightarrow$modulation delay

T_p $\rightarrow$ Pulse duration

T_c $\rightarrow$ Frame repetation time

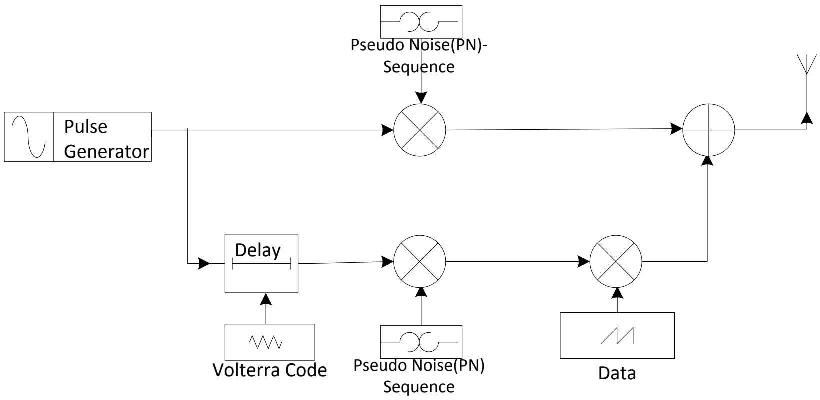

Fig. 2.2. Block Diagram of TRDH-Transmitter

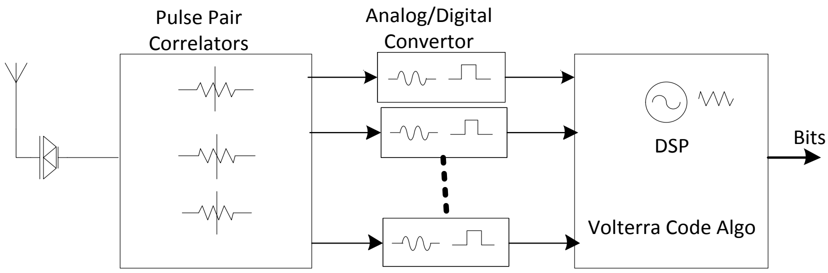

Fig. 2.3. Block Diagram of TRDH-Receiver.

The received signal can be defined as [13]

$$s^{TRDH}(t) = \sum_{i=0}^{\frac{N_p}{2}-1} \sqrt{\frac{E_b}{N_p}}\ \omega(t - iT_c - gd_k\, D) + \sqrt{\frac{E_b}{N_p}} a_k\, \omega(t - iT_c - T_m - gd_k\, D) \quad (2.1)$$

In case of BPPM (binary pulse position modulation), D (modulation delay) is less than T_c $D < T_c$, and T_m $is\ minimum\ delay\ between\ two\ pulses$ $(doublet)$. So as to avoid IPI(inter pulse interference) and ISI (inter symbol interference), T_c and D are set with different values.

"g" is a variable used for receiver and its value is 1 for TRDH (g will be zero for RAKE receiver). Subsequent will be the received signal in case of RAKE [14].

$$s^{RAKE}(t) = \sum_{i=0}^{NP-1} \sqrt{\frac{E_b}{N_p}} a_{k\,,} i\omega(t - iT_c - d_k\, D) \quad (2.2)$$

For the said signals' structures defined in above equations, the symbol (energy) is correspondingly spread over N_p (pulses putting together a symbol)

The received signal => $r(t) = s(t) * h(t) + n(t)$, (2.3)

'*'= continuous time convolution. $h(t)$ = impulse response. $n(t)$ = white Gaussian random value. To compare the effectiveness of TRDH with RAKE an Additive white Gaussian noise "AWGN" channel is used (With the assumption that there is no IPI and ISI [15])

2.2 *BER* Performance

For the Transceiver’s performance evaluation, *BER*/*SNR* model was simulated under MATLAB. The *BER* performance of the proposed TRDH architecture was analysed with traditional RAKE architecture[16] , for this purpose, the author has measured the output of the correlator as Gaussian, so that the bit error rate can be signified as tail probability (Q-Function), using the Signal to Noise Ratio (*SNR*) formulation for Transmitted Reference .

$$BER_{\mathrm{TRDH-BPPM}} = Q\left[\sqrt{\frac{\frac{2E_b}{N_O}}{(4+2g+2N_{\mathrm{p}}2TW\frac{N_O}{E_b})}}\right] \tag{2.4}$$

$$BER_{\mathrm{TRDH-BPAM}} = Q\left[\sqrt{\frac{\frac{2E_b}{N_O}}{(4+N_{\mathrm{p}}2TW\frac{N_O}{E_b})}}\right] \tag{2.5}$$

For RAKE Receiver

$$BER_{\mathrm{RAKE-BPPM}} = Q\left[\sqrt{\frac{\frac{2(N_{\mathrm{p}}-1)E_b}{N_{\mathrm{p}}N_O}}{4\frac{N_{\mathrm{p}}}{N_{\mathrm{p}}-1}-\frac{6}{N_{\mathrm{p}}-1}(N_{\mathrm{p}}2TW\frac{N_O}{E_b})}}\right] \tag{2.6}$$

$$BER_{\mathrm{RAKE-BPAM}} = Q\left[\sqrt{\frac{\frac{2(N_{\mathrm{p}}-1)E_b}{N_{\mathrm{p}}N_O}}{4\frac{N_{\mathrm{p}}}{N_{\mathrm{p}}-1}-\frac{6}{N_{\mathrm{p}}-1}(N_{\mathrm{p}}TW\frac{N_O}{E_b})}}\right] \tag{2.7}$$

2.3 Simulation Results

In order to understand the behavior of proposed radio architecture, performance is compared with RAKE architecture Figure 2.4. In the first test, *BER* is plotted versus *Eb*/*No* (the energy per bit to noise power spectral density ratio). From the simulation results, it can be perceived that TRDH performs well in both modulations BPPAM and BPAM cases. Overall TRDH-BPAM performance is slightly better than TRDH-BPPM.

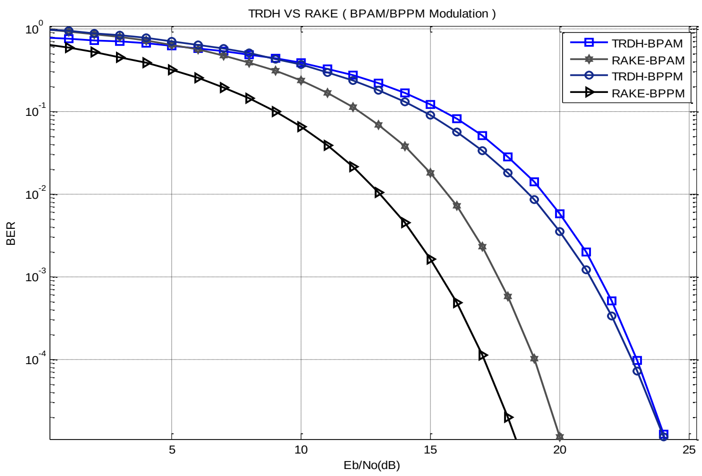

Fig. 2.4. ***BER* for N_{p} = 15 for *TW* = 150 and *Eb*/*No* = 20 dB.**

RAKE-BPPM performance is lowest. RAKE-BPAM performs better than RAKE-BPPAM, at a *BER* = 10^{-4}, the RAKE-BPPM system performance is less than 2 dB (less than the worst case of TRDH).

In Figure 2.5, *BER* vs. N_p (no of transmitted pulses) is plotted. The TRDH-BPAM and TRDH-BPPM both provide better performance. The performance of RAKE decreases when N_p increases. The RAKE-BPPM/BPAM structures are severely inclined by the pulse repletion structure.

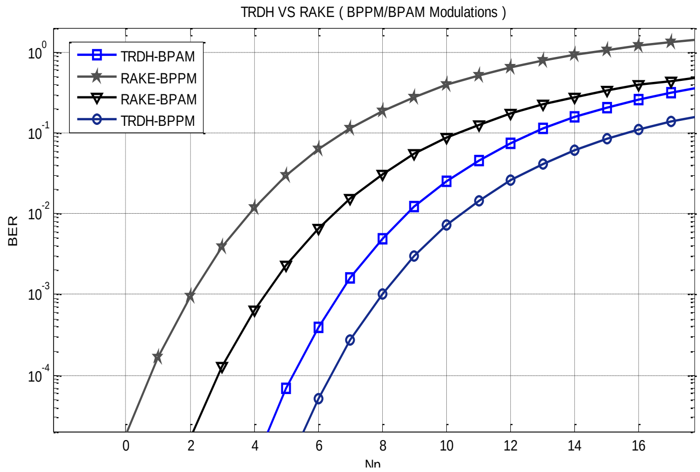

Fig. 2.5. *BER* vs. N_p for *TW* = 150 and *Eb*/*No* = 20 dB.

In Figure 2.6, *BER* performance against *TW* (time-bandwidth product) is plotted. TRDH-BPAM and BPPAM both show better performance at low TW values, RAKE-BPPM is slightly far from the TRDH in terms of performance. Similarly, the RAKE (BPPM) slightly outperform the TRDH systems due to an abridged number of signal-noise cross terms that states the decision variable.

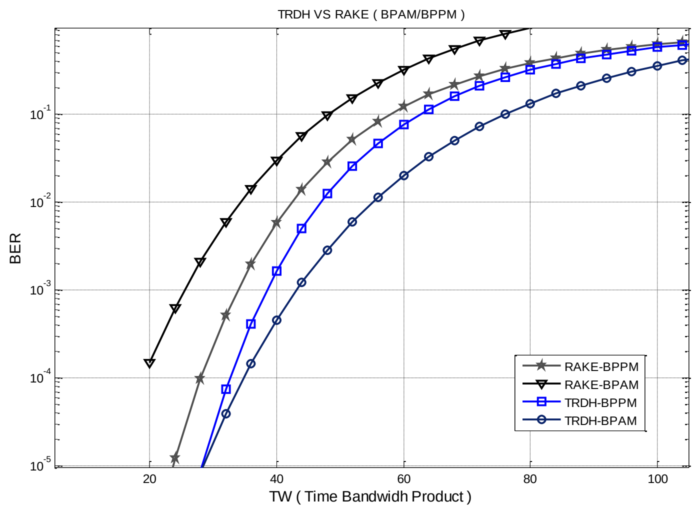

Fig. 2.6. *BER* vs. N_p for *TW* = 150 and *Eb*/*No* = 20 dB.

Figure 2.7 shows results of an additional test to check the *SNR* vs. *TW* performance of both schemes. As expected, TRDH gives high *SNR* even at a higher number of *TW*. For example, both TRDH (BPAM and BPPM) are giving *SNR* > 20, while *TW* was over 70. On the other hand, RAKE-BPAM gives *SNR* about 25 but for the *TW* < 40.

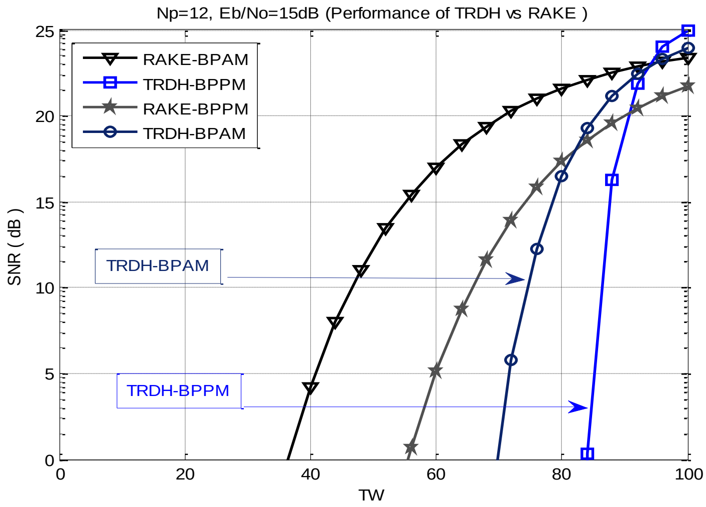

Fig. 2.7. *SNR* vs. N_p for *TW* = 150 and *Eb*/*No* = 20 dB.

3. Clustering based Adoption features

The cluster formation is based on a transmission range rule, where groups are formed based on transmission range from the base station. Additionally, a threshold level is fixed for the cluster membership, and the number of members for a cluster never cross that limit. Beside this cluster head selection is based on multiple parameters called cost function [17]. That selects the strongest node as a cluster head. These two major enhancements not only simplifies the network formation but also improves the overall network performance.

3.1 Proposed Strategy

In our technique, adoption is divided into two parts; Formation-phase and Stabilize-phase. Formation phase focuses on cluster setup and CH selection, whereas data transmission and routing are managed in stabilize-phase. Following are the major steps (with some assumptions).

- Nodes are deployed randomly across the target region.
- At the start of the simulation, all nodes have the same amount of energy.
- All nodes have the ability to transfer data to any other node or to the BS (base station).
- IR-UWB is used at radio layer.
- Channel characteristics are symmetric (transmission power for a message from the *x* node to the *y*, ($x \rightarrow y$) node is same as ($y \rightarrow x$).

3.2 Formation Phase

Cluster Formation & CH Selection: Here nodes are divided into groups based on their transmission range from the base station. To restrict the number of nodes; a threshold level is defined. CH will not exceed the membership of nodes (as described by threshold level). Following are thigh level steps.

- At start up, the base station collects the information of all the nodes.
- On reception of the pilot, every active node; sends the basic details such as node id, energy level and distance to the base station.
- Based on the received data, factions or groups are derived Figure 3.1. Accordingly CH is selected from the available candidates.

Faction are based on the transmission range from the BS. (Nodes within base station's T_x range are Faction (1) and faraway nodes are defined in higher level (e.g. Faction (2) and so on.

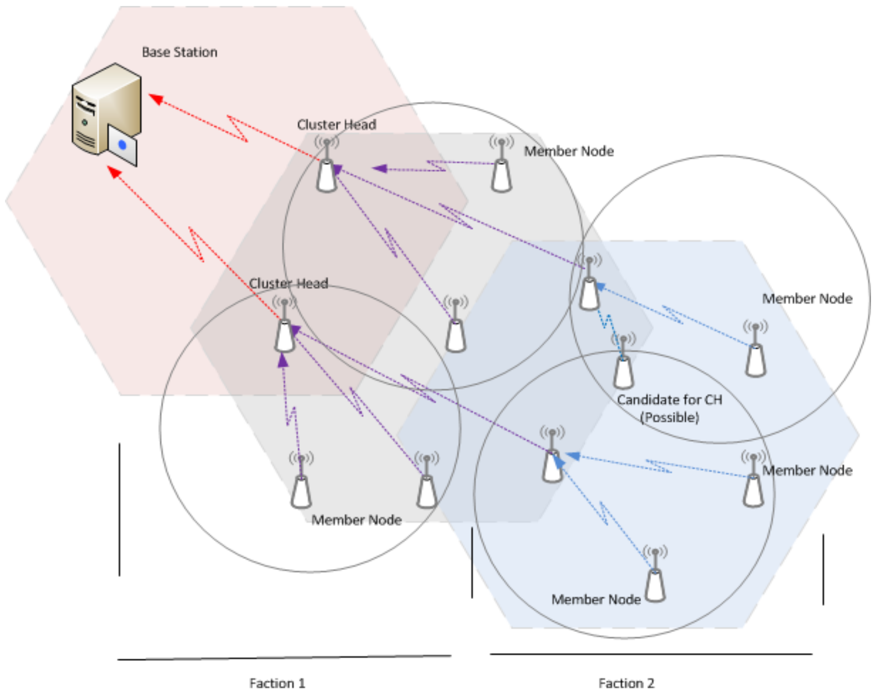

Fig. 3.1. Faction based Clustering Technique.

After the selection of CH, schedule is created and shared with the member nodes. Following are the main steps involved here.

1. Data sensing process starts.
2. Based on the activity when data is sensed and gathered the nodes wait for their turn and transmit data to CH (according to defined MAC schedule)
3. At the end of the cycle, CH performs aggregation process and transfers data to the BS.

3.3 Stabilize Phase

During this phase, each cluster manages its data gathering and routing schedule by using MAC algorithm [3]. Stabilize phase carries two important communications, communication within the cluster, and communication with the sink (& other CHs). Figure 3.2 explains the design of stabilizing phase of our proposed method. In order to avoid the interference between these two communications, different channels are allocated to each cluster. That is shared with the member nodes of each cluster by CH. CH gets this information from BS during formation phase.

3.4 Intra-Cluster Communication

After the cluster formation, member nodes collect data, and according to the mac-schedule forward it to the cluster head. Cluster head assembles (collected) data and performs aggregation. At the end of this step, data is forwarded to the base station (via neighboring cluster head or direct to BS) see Figure 3.2. All members of clusters use a unique channel number which is shared via CH. This protects the interference from neighboring cluster.

3.5 Inter-Cluster Communication

Each cluster head designs the communication schedule based on the Pilot signal Assisted-MAC, it is a multi-phase algorithm explained in [3]. See Figure 3.2 showing both types of communications with the logical paths. CH to CH communication or CH to BS communication uses a separate channel (different from the inter-cluster communication channel) which does not interfere with the inter-cluster communication.

3.6 Interference Management

Here, the common interference issue, 'Near-Far effect' is managed by two-step inference management, where radio/physical layer (thoroughly described in chapter 2), and the MAC Layer both works together. This cross-layer structure creates communication stability and reduces interference effect. Addition to this for the inter-cluster communication interference, the coding technique (the Volterra Model [18] protects the communication from internal interference.

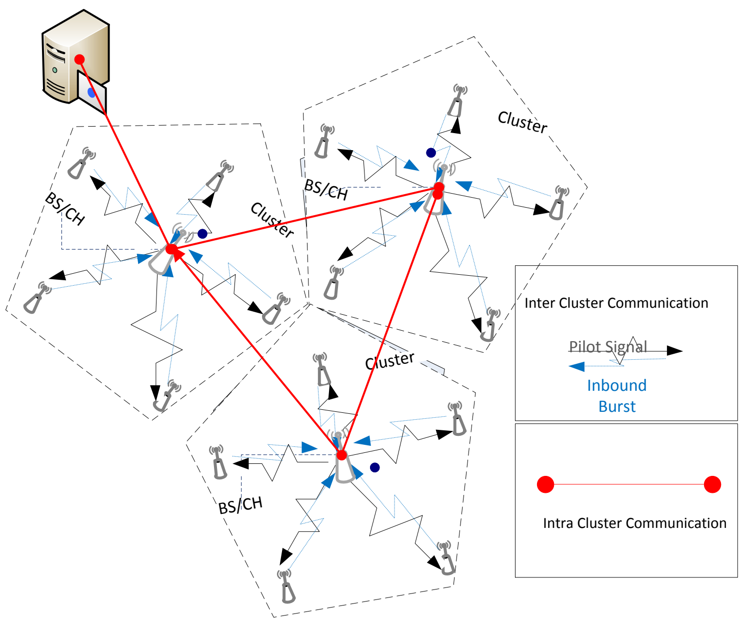

Fig. 3.2. Intra & Inter-Cluster Communication.

3.7 Simulations & Performance Evaluation

Starting with the experimental design (and for performance matrices) MixiM (under OMNET++) for the overall modeling is used. Table 3.1 shows the core parameters and their values used in the simulation.

Table 3.1. Simulation parameters and corresponding values

Parameters	Values	Parameters	Values
Network Area (m)	100 × 100	Pulse Duration	5 ns
No. of Nodes (n)	100	No. of runs	50
Initial Energy (of nodes)	1 J	ε_{fs}	250 pJ/b
$\boldsymbol{E_{\text{elec}}}$	5 nJ/b	d	50 m
Datagram	4 Kbits		

3.8 Average Energy

A method to check the effectiveness of an optimization technique is to calculate the average energy consumption. For the energy consumption of the transmutation of an x-bit is derived from [6]

$$E_{\text{TOT}}(i) = E_{\text{Tx}} + E_{\text{Rx}} \qquad (3.1)$$

E_{TOT} is the total energy consumed by the node 'i'. E_{Tx} is the energy consumed at the transmitter end and it's given by

$$E_{\text{Tx}}(b, d) = (E_{\text{elec}} \times b) + (\varepsilon_{\text{fs}} \times b \times d^2) \qquad (3.2)$$

Similarly E_{Rx} are receiver's consumption and its equal to

$$E_{Rx}(b) = E_{\text{elec}} \times b \qquad (3.3)$$

E_{elec} is the expanded energy (of radio) and it is assumed that during the formation phase nodes are aware of each other's location. The datagram packet size is fixed to 4 Kbits. When the battery life of a node depletes to "zero" it is considered dead.

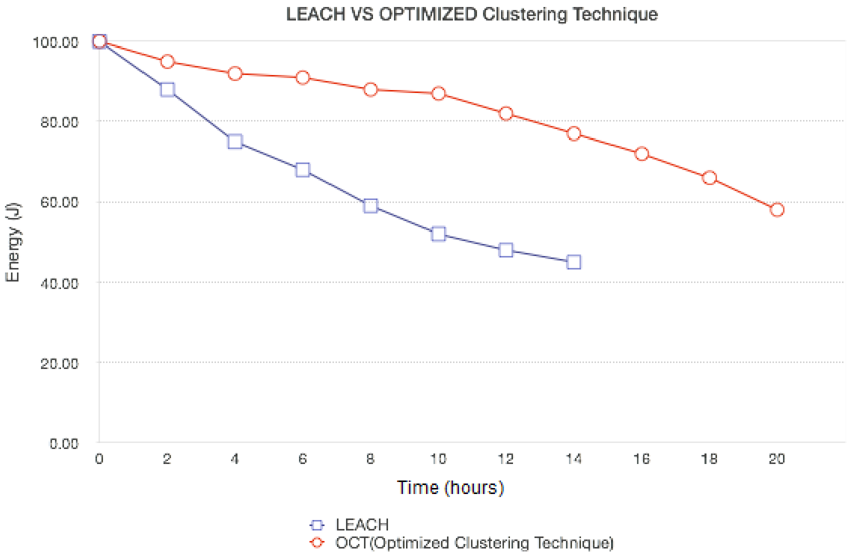

Figure. 3.3. Energy Consumption (LEACH vs. OCT).

From the simulation results in Figure 3.3, it can be seen that by applying clustering technique residual energy is improved even in a dense network case (n = 100). By comparing with LEACH and OCT, one can see that, after the 14th hour; for the same value of n, Leach has about 40 Jules energy (left), on the other hand, OCT has about 75 Jules. OCT excels in both energy and packet delivery. There are many factors behind this, cross-layer coordination, synchronization and most important CH selection technique are the major success factors.

3.9 Lifetime of the Network

The lifetime of a network is directly proportional to the lifetime of its nodes. Which in fact depends on the succession of packet delivery. Increase number of jamming during data transmission or packet drop during a session can put the repetitive burden on the network flow that consumes lots of additional energy. Hence affects overall network performance.

Figure. 3.4 Network Life-Time Analysis

During the simulation, network size was increased gradually (n = 5 nodes to n = 100). It was observed that the network lifetime remains between 6 and 9 hours (which is very stable figure).

By increasing the number of nodes, lifetime of network also increases. Technically that is true because energy burden is divided among nodes. By looking at the graph, network lifetime was on its peak when $n = 100$. Which is biggest "n" value. That means OCT has resolved the issue (Pilot assisted MAC performance under dense network) where network performance drops when $n > 20$. From simulation analysis, OCT gives the same level of performance as LEACH. Just to make sure that results are accurate, experiments are repeated multiple times. The optimized clustering scheme has smooth performance in case of network lifetime see Figure 3.6. One of the reasons for such improvement is due to the use of cost function. Where not only energy but also other factors are also considered.

3.10 Packet Delivery Ratio

Ratio is the calculated on the basis of the following formula,

"Percentage of successfully transported packets = Total No. of Received packets / Total No. of Transmitted packet".

From Figure 3.5, it is observed that the optimized clustering approach has better packet delivery value than LEACH also performance is consistent even when the number of nodes is high .e.g. $n = 100$). That proves the success of PA-MAC in a dense network environment. It is also observed that as the number of nodes increases, the packet delivery ratio improves. This is because more nodes mean more options for direct connectivity with BS and more candidates for the cluster head. From Figure 3.5, we can observe that more packets arrived on the base station when optimization techniques (i.e. OCT) is used.

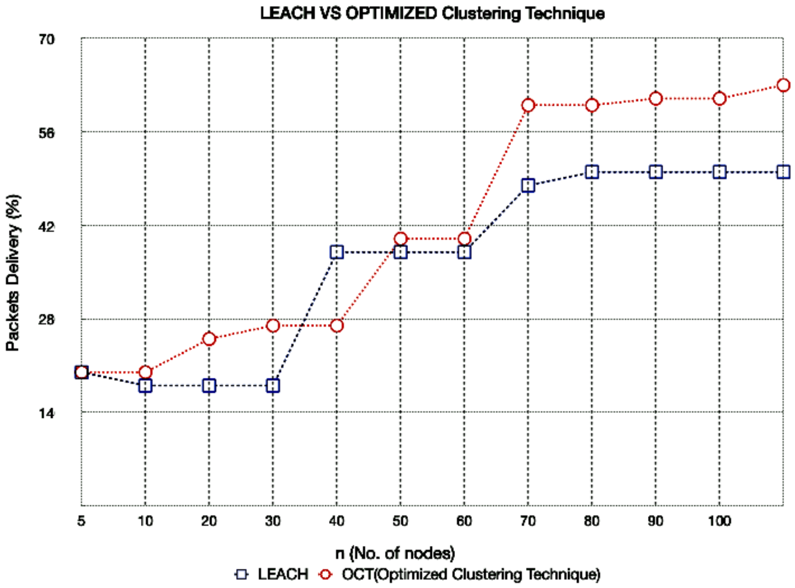

Figure. 3.5 Packet Success delivery Ratio

4. Analysis of Self-Healing Capability of IR-UWB based PA-MAC Framework

After the implementation of TRDH architecture in our framework, the network performance was very good for the small indoor networks, but when performance was tested under the dense network conditions, network lifetime was seriously affected. To rectify this issue I applied some adaption features, e.g. clustering. The main goal of this chapter is to evaluate the "Self-Organizing capability" of our framework after the adoption optimization.

Here the same system and Network models are used as our previous chapter [19]. Hence, the MAC and the PHY processes are the same.

4.1 Energy Model

The energy model of the framework is derived from [19][20], where the network has a variable size from 100 to 500 nodes (for each scenario). The coverage area for nodes deployment is 100 × 100 square meters. Figure 4.1.

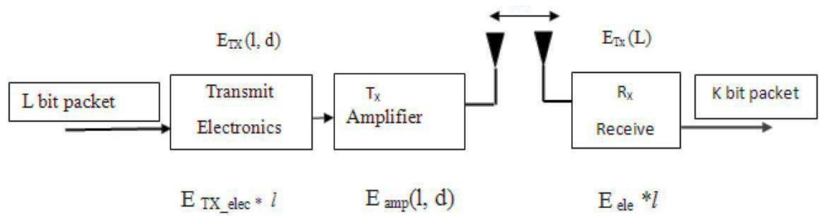

Fig. 4.1. Energy Model of the proposed framework [20]

Energy model shown in Figure 4.1 is used for the energy dissipation [20]. Free space (d2) is used for the distance/energy corresponding between the source and destination nodes. Similarly, for the multi-path fading effect (d4) channel models are considered. Energy used for the transmission of x bit can be calculated from the following equation [21].

$$E_{\mathrm{TOT}}(i) = E_{\mathrm{Tx}} + E_{\mathrm{Rx}} \tag{4.1}$$

Where E_{TOT} is the total energy used at 'i' and E_{Tx} is transmission energy at the transmitter

$$E_{\mathrm{Tx}}(b, d) = (E_{\mathrm{elec}} \times b) + (\varepsilon_{\mathrm{fs}} \times b \times d^2) \tag{4.2}$$

In the same way E_{Rx} is the energy at the receiver's end

$$E_{\mathrm{Rx}}(b) = E_{\mathrm{elec}} \times b \tag{4.3}$$

E_{elec} is (radio's) expended energy. Default packet size is = 4 Kbits (Amount of data any node wants to transmit to CH varies as per pseudo-random code) When nodes energy reaches to "zero". It will be disconnected from the network.

4.2 Self-Organizing Capability

The self-organizing capability is an important feature of wireless sensor networks[22]. It improves scalability and auto adaption to changing network conditions [23]. Network's ability to auto adjust its topology in case of environmental changes is the key idea behind self-organization. Self-organizing capability cooperates with the network topology and provides stability. The self-organization's flow diagram is defined in Figure 4.2.

Scenario 1: Death of a single (randomly selected) node.

I started our evaluation with the simplest case, where single (random) nodes are selected, and its battery's energy was changed to "zero". Means node went down Fig. 4.3 (a).

Scenario 2: Death of a CH in a random order.

In this scenario, the author has randomly selected cluster head and changed its battery energy to "zero".

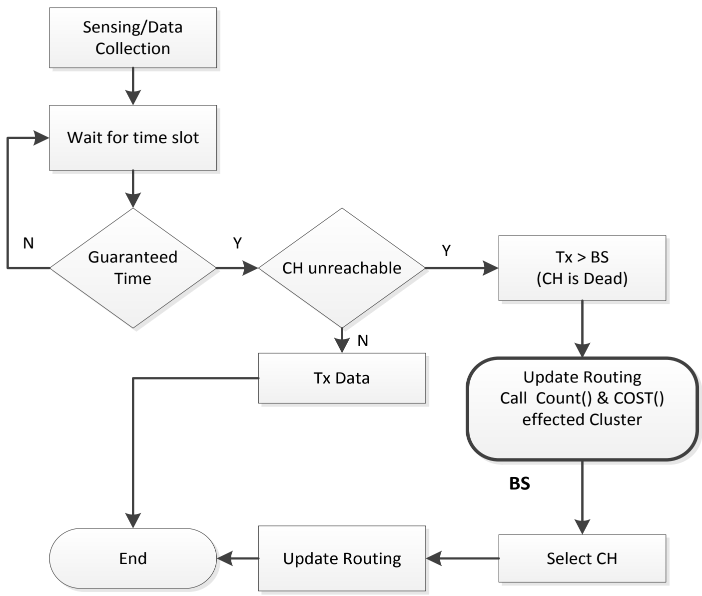

Fig. 4.2. Self-Organization flow diagram.

In order to get more accurate results, the scenario was repeated multiple times with the different numbers of CH Figure 4.3 (b).

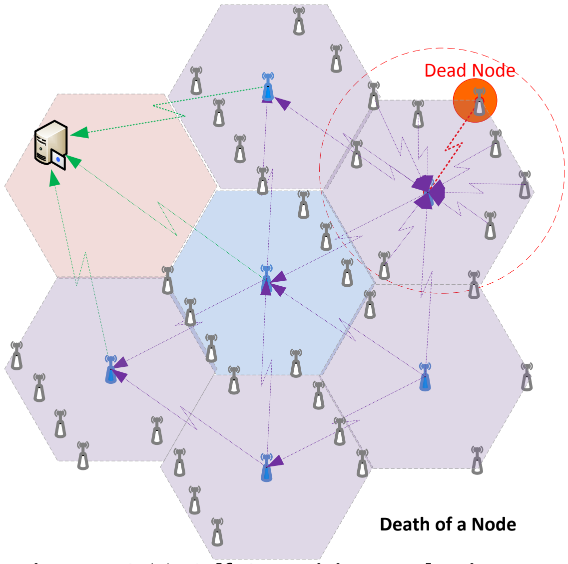

Figure. 4.3 (a). Self-Organizing Mechanism.

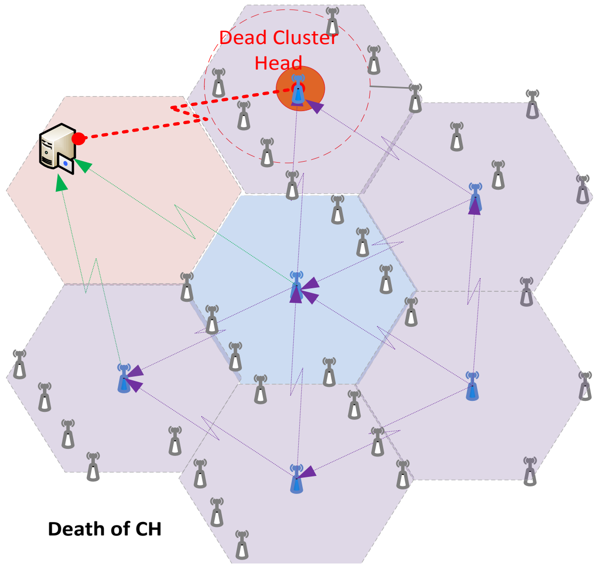

Figure. 4.3 (b). Self-Organizing Mechanism.

Scenario 3: Death of CH and a node at the same time. In this scenario, the author has brought down one node as well as the cluster head. I repeated the scenario with multiple cases, e.g. selection of CH and node from the same cluster, CH, and node from two adjacent clusters, CH and node from two randomly selected clusters, etc. Both random and manual ways were used, Fig. 4.3(c).

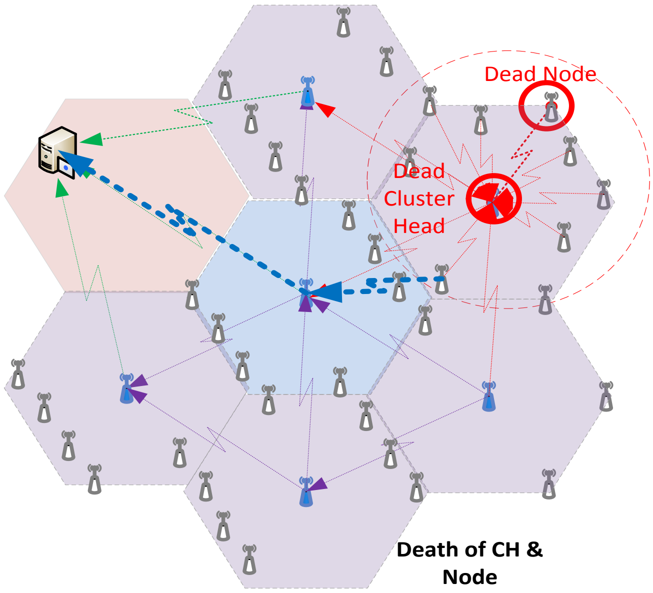

Fig. 4.3 (c). Self-Organizing

4.3 Simulations & performance evaluation

Omnet++ simulation platform [24] is used for the evaluation of our framework. Parameters used in the simulation are given in Table 4.1. The simulation was executed for the multiple scenarios where node count was from 100 to 500.

Table 4.1. Simulation Parameters

Parameters	Values
Network Area (m)	100 × 100
No. of Nodes (n)	100–500
Initial Energy (of nodes)	100 J
$\boldsymbol{E}_{\mathbf{elec}}$	5 nJ/b
Datagram	4 Kbits (default)
Pulse Duration	5 ns
No. of runs	50–100
$\boldsymbol{\varepsilon}_{\mathbf{fs}}$	250 pJ/b
D	50 m

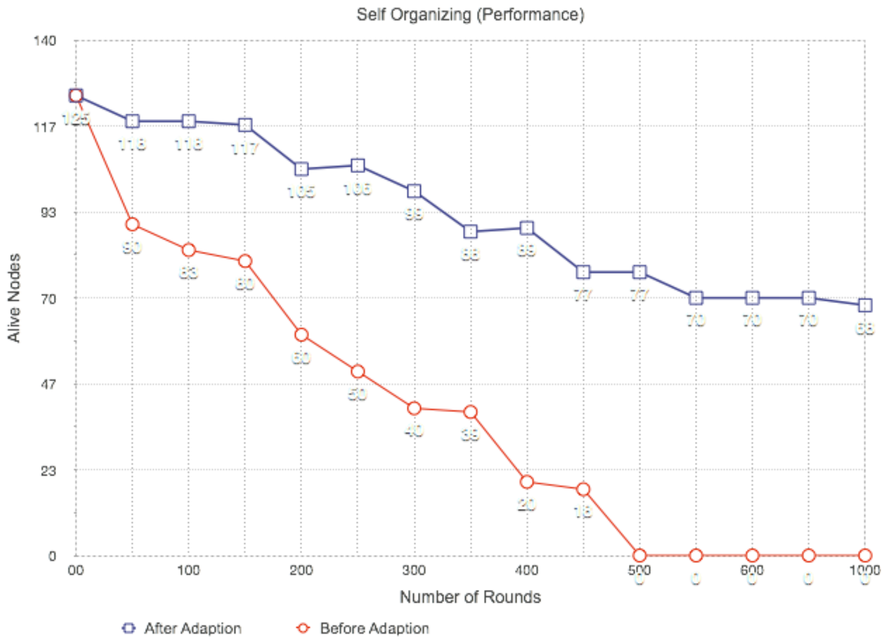

Fig. 4.4. Network Lifetime before & after Adaption.

Following evaluations are drawn for the performance of self-organizing feature of our architecture. Here the author has examined the network lifetime of the proposed framework, before and after applying adaption features. Looking at the Table 4.2 and Figure 4.4: before adoption, HND (half nodes death) was at 152nd round. On the other hand, after the implementation of adoption, HND was noticed at 890th round. That is over 60 % improvement in the network lifetime. By looking at the comparison between "packet delivery before adoption" and packet delivery after adoption" Table 4.3.

Table 4.2. Network Lifetime

S#	Scenario	1st Node Death	HND	% Improvement (Lifetime)
1	After Adaption	45	890	59.23
2	Before Adaption	4	152	NA

Table 4.3. Delivery Ratio

S#	Scenario	% Delivery Ratio
1	Before Adaption	15 %
2	After Adaption (Regular)	95 %
3	At 1 CH-Death	65 %
4	At 1 Node Death	90 %

It can be observed from the table that before adoption, the packet delivery ratio was seriously affected, and the success ratio was just 15 %. After implementing adaption features, there is a significant improvement, and the packet delivery ratio increased to 95 %. Similarly for the 1 node death case, performance was slightly down to 90 %. But when a cluster head went down, performance decreased to 61 %. That's logical as the death of cluster head impacts the whole network. Comparative analysis of energy consumption shows that before the implementation of optimization strategy, remaining energy was 34 J at 50th round and at 800th round it dropped to 0.057 J. On the other hand, remaining energy at the 1000th round for CH death case was 2.1 J, and for 1 node death and regular case about 8 J/s. That is a significant improvement in terms of energy, see Table 4.4.

Table 4.4. Remaining Energy

S#	Scenario	Total Energy (remaining)
1	Before Adaption	0.045 J/s
2	After Adaption (Regular)	8.124 J/s
3	At 1 CH-Death	2.183 J/s
4	At 1 Node Death	7.782 J/s

5. SMART Incubator: Implementation of PA-MAC Framework in WBAN

A project called “SMART Incubator” (Smart incubator is a life-saving baby bed (capsule) for premature newborn babies) was initiated for the practical evaluation of our framework. In this research UWB, based PA-MAC architecture is used by a WBAN application.

A complex, heterogeneous sensor network testbed was set up with some basic monitoring sensors, e.g., ECG, SPO2, body movement, and temperature. The network topology is divided into two segments (or clusters); a static network based on 13 fixed nodes (installed in the incubator), and a dynamic network of 9 (attachable) nodes (all connected to a human body). The major role of the static network segment is to capture environmental conditions, e.g. humidity, air temperature, and light. Whereas BAN-based network is used for the core body readings. Both network segments feed their sensed data to a central base station (coordinator node) via a router node (Cluster Head). At the application layer aggregated data are used for medical purposes. network modules is defined.

Fig.5.1. MAS WBAN Experiment kit: (a) wireless perspiration sensor; (b) Coordinator Node (c) Application Layer.

5.1 Architecture with Basic Building Blocks

The high-level network architecture is based on two major segments Figure 5.2.

1- Static Network Cluster (Fixed nodes installed in the Incubator).

2- Dynamic Network Cluster (BODY-based nodes installed on different body parts).

Each network cluster has a CH, which functions as a router node. Both CH is connected to a central BS, who works as a coordinator node, and consolidates the sensed data (which is used by Application Layer). Data transmission between the nodes, and to base station uses UWB as a media channel. Each node has two major parts: Sensing circuitry, and a transceiver circuitry.

The data rates of different sensors are given in Table 5.2.

Unlike a normal WSN monitoring network, Smart Incubator's operational function is very critical, as it has to operate consistently with high accuracy under severe conditions (e.g. first 48 hours of a premature birth). Therefore, reliability and consistency of sensory signals are crucial.

Node Architecture

MAS WBAN kit Figure 5.1, provides flexibility to use different kinds of nodes structures. After thorough study and considering SMART Incubator project's requirement an amplifier based node architecture [25] is selected Figure 5.3. Functionally in such a design, the narrow baseband pulses are filtered using a band pass filter (3.5 GHz to 6.5 GHz). The UWB pulses are then amplified using a wideband low noise amplifier (LNA) to meet the –41.3 dBm transmission power level. This amplifier has been included to guarantee that the amplitudes of the UWB pulses are sufficient to provide a targeted coverage of the application (name as MAS control).

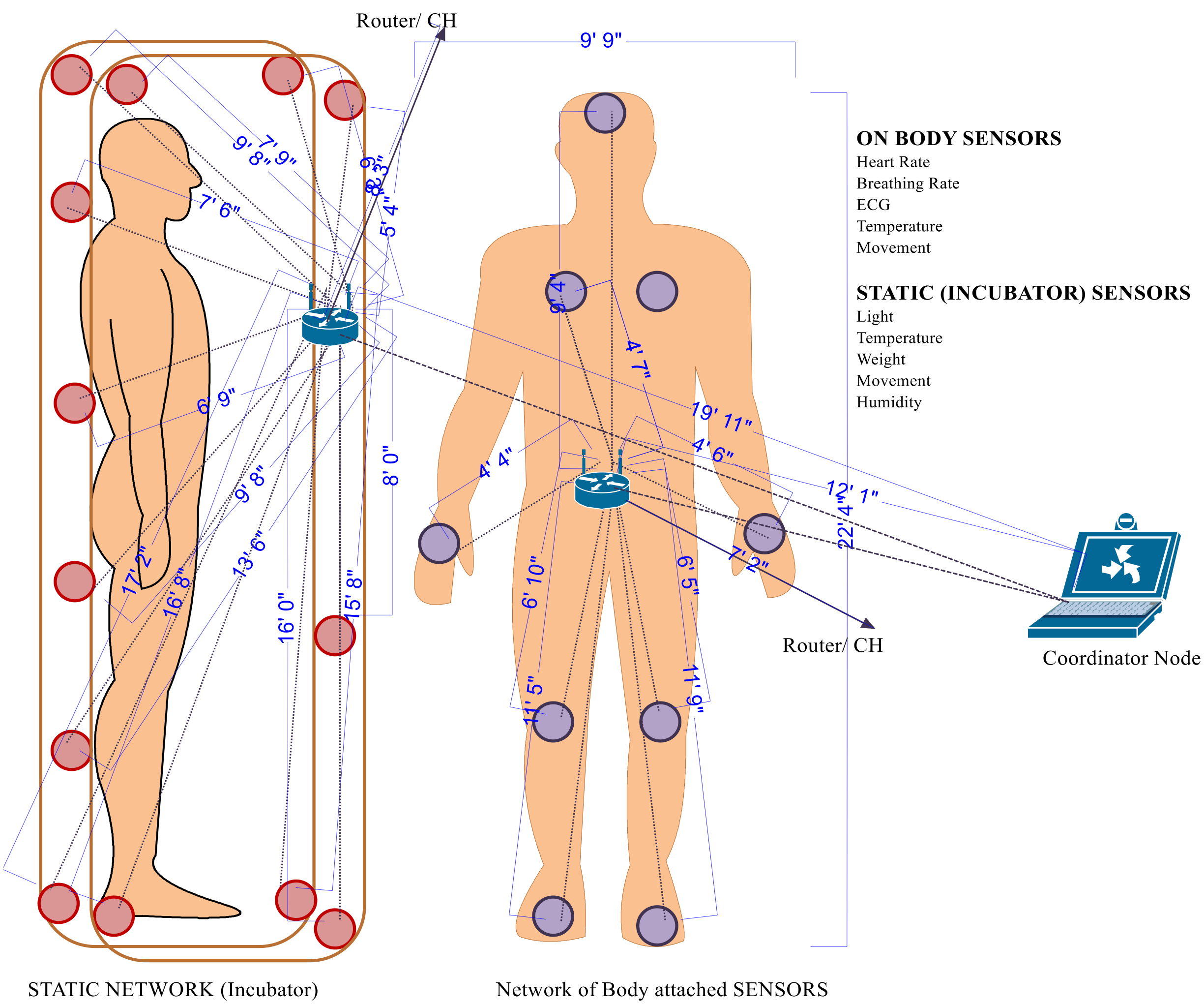

Fig.5.2. Static network segment and dynamic nodes network segment of SMART Incubator.

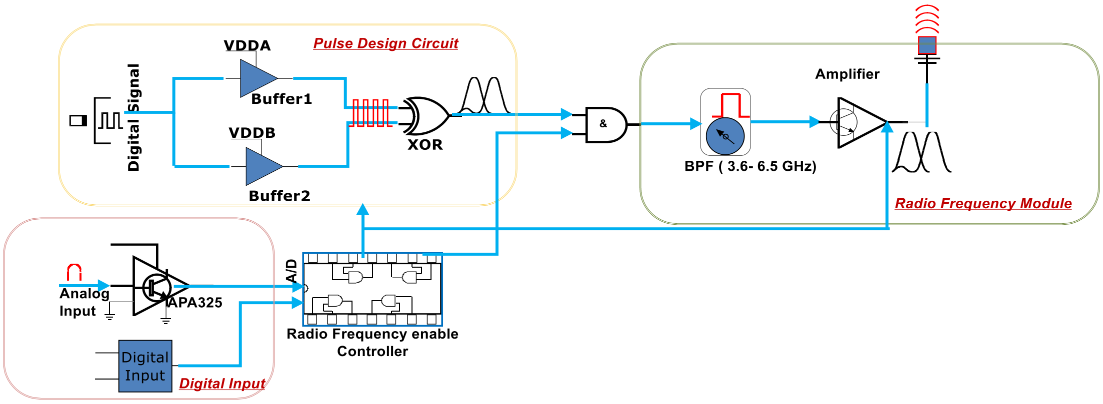

Fig.5.3. Node Architecture used in the MAS - Experiment kit.

The power spectrum consists of several frequency lobes spread throughout the UWB bandwidth. The amplitudes of these frequency lobes decrease towards the upper part of the UWB spectrum. The UWB sensor node transmits UWB signals in the band of (3.8 to 4.5) GHz. The amplitude of the frequency lobe within the (3.8 to 4.5) GHz band is well below the maximum allowable power level by the FCC (–41.3 dBm/MHz) [26]. The node design employs two amplifier stages to boost the power level of the transmitted UWB signal within the band of (3.8 to 4.5) GHz (as marked in Figure 5.5) while containing the power level within the FCC spectral

5.2 Transceiver Architecture

The underneath transceiver architecture used in the experiment is based on DHTR (Delay hoped transmitted reference) [2]. Figure 5.4 shows the schematic way of doublet's operations in DHTR. Here pulse repetition time (PRT) of doublet (i.e. delay) may be varied as per the spectrum. Figure 5.4 Transmitted Reference receiver works by measuring correlations [27]. Delay hoping is delayed modulation and used for multiple access [28].

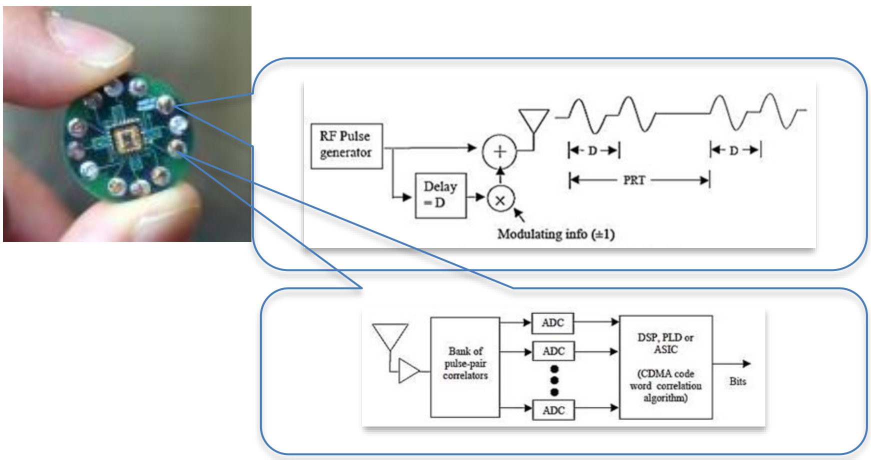

Fig. 5.4. HLD (High-Level Diagram) of DHTR Transceiver.

High-level design of DHTR is explained in Figure 5.5. It has a series of pulse-pair correlators linked from side to side to LNA to an antenna.

Each correlator works on a different delay. Next to correlators is a Volterra code [12] word correlator. Correlation is dealt in firmware as DSP under programmable logic device (PLD) and ADC samples the output of doublets.

The correlation process is an analog process based on delay, multiplexer, and integrator. Each signal is divided into two paths, where the 2nd is an exact signal, but with some delay[29]. In the end, both are multiplied, and the output is integrated on a chip time.

5.3 UWB Reception

The HLD (high-level diagram) of the receiver is shown in Figure 5.4 [2][30]. It can be seen that Band Pass Filer confines the received signal in the range of 3.2 GHz to 5.6 GHz. After the filtering, amplification is applied by using multiple LNAs that amplifies the signal by 50 dB. The amplified baseband signal is further processed by Mixer and Voltage Control Oscillator on the received signal spectrum right after the antenna and afterward the LNA stage Figure 5.5. At the next stage, the output signal from Mixer and VCO passes through a Low Pass Filter for the integration, this step enables the baseband signal to be amplified by ADC. The role of Low Pass Filter is to stretch the pulses as per ADC detection range. Output signals (e.g. from Mixer and Low Pass Filter) can be seen in the following figure, Figure 5.5.

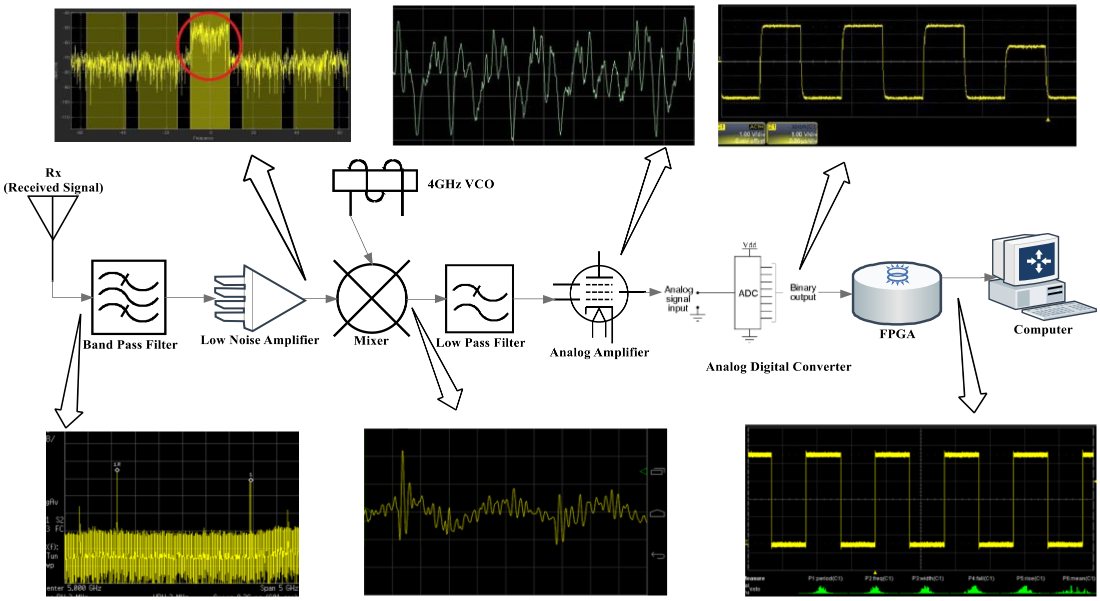

Fig. 5.5 Step-by-Step outputs of TRDH UWB receiver.

Analog amplification brings the UWB signal in a recovered state, which passes through an analog-digital converter and finally by field programmable gate array (FPGA). This is the last stage of a UWB pulse reception. Field programmable gateway array has a straight forward role just to digitize the received pulse in a binary manner.

Here data transmission was controlled by the PA-MAC (Pilot Signal Assisted- MAC) defined in Chapter 2, [3].

Our test kit “MAS WBAN” is integrated with LabView [31] and MATLAB [32], so simulation results can easily be compared with real received date by experiments.

Experiment Setup

Experiments were executed by an agile approach [1], where static and dynamic (body network) segments were tested separately and once successfully configured, coordinator nodes connect both segments. All results were finally compared with simulation results. See following graphs for the detailed network behavior.

Propagation Channel Model

$$P_{\mathrm{dB}}(d) = P_{0,\mathrm{dB}} + a(d/d_0)^n + N\big(\mu(d), \sigma^2(d)\big) \tag{5.1}$$

$$h_i(t) = M_i \sum_{u=0}^{K} b_{u,v}^{i}\, \delta\big(t - T_u^i - \tau_{u,v}^i\big) \tag{5.2}$$

$$h_i(t) = M_i \sum_{u=0}^{K} \sum_{v=0}^{L} b_{u,v}^{i} \delta\big(t - T_u^i - \tau_{u,v}^i\big) \tag{5.3}$$

here M_i is lognormal shadowing, $b_{u,v}^{i}$ are the coefficients for the multipath gain. T is time delay for “*u*” the UWB pulse.

I derived this from [12], assuming “*d*” as a distance, Average path loss will be

$L1 = 20\log(\frac{4\pi f_c}{c})$, $L2 = 20\log(d)$ and $L = L1 + L2$.

Where " f_c "represents the central frequency, and $d = 1$ m for all experiments.

Experimental Parameters

For the performance measurement following formulas and key parameters are considered.

$$PL = \frac{L}{S} \tag{5.4}$$

$$D = T1 - T2 \tag{5.5}$$

$$Throughput(\%) = \frac{R}{C} \cdot 100\ \% \tag{5.6}$$

$$E\left(\frac{\mathrm{J}}{\mathrm{bit}}\right) = \left(\sum_{i=0}^{K}(I(\mathrm{A}) \cdot V(\mathrm{V}) \cdot T_{\mathrm{tx-rx}}\,(\mathrm{s}))/\sum_{i=0}^{K} B\right) \quad (5.7)$$

Here "*R*" is bit-rate (in bps), "*C*" is capacity (in bps), "*S*" is a number of transmitted packets, "*E*" is energy and "*PL*" is packet loss.

Table 5.1 defines core parameters.

Table 5.1. Key Parameter values used in SMART Incubator

Parameter	**Value**
Total number of static nodes	13
Total numbers of body (dynamic) nodes	9
Periodic traffic nodes	6 (body)
UWB-Frequency	3.2–5.6 GHz
UWB TX (power)	1.5 mW
UWB Rx (power)	15 mW
Sleep mode (power)	0.25 mW

Performance Constraints

For the performance evaluation same scenarios, executed on simulation tool were repeated on MAS-WBAN hardware kit. In the end, both simulation results and hardware findings are compared. In test scenarios, CH has been assigned more power than a regular member node, so it can store data, forward it to BS, and creates MAC schedules for member nodes. Data rates were used as per the table 5.2.

Table 5.2. Major Sensing Parameters

Parameter	**Function**	**Tx-cycle**	**Data-rate**
ECG	Heart rate monitoring	Continuous	2.8 kbps
SPO2	Respiration rate	Continuous	1.1 kbps
Temp	Temp inside Incubator	Every 2 s	15 bps
Humidity	Humidity inside incubator	Every 5 s	10 bps
Notch	Body movement	Every 1 s	5 bps
Light	Light in incubator	Every 1 min	2 bps

For the continuous sensing nodes, nodes have seven bytes of overhead and 550 bytes of payload. That can be transmitted in one clock slot (as per MAC). On the other hand, for the periodic sensing, the packet is based on 5 bytes of overhead and 43 bits of payload.

5.4 Performance Analysis (Simulation vs. H/W)

For the detailed analysis, readings are collected from both Simulation tool and hardware toolkit.

Packet Loss Ratio

Packet loss in WBAN communication has two major reasons, communication collision due to the weak MAC strategy, and interference [33]. Due to resource limitations, a limited number of nodes were deployed in both static and dynamic networks. Hence, some collisions were not high.

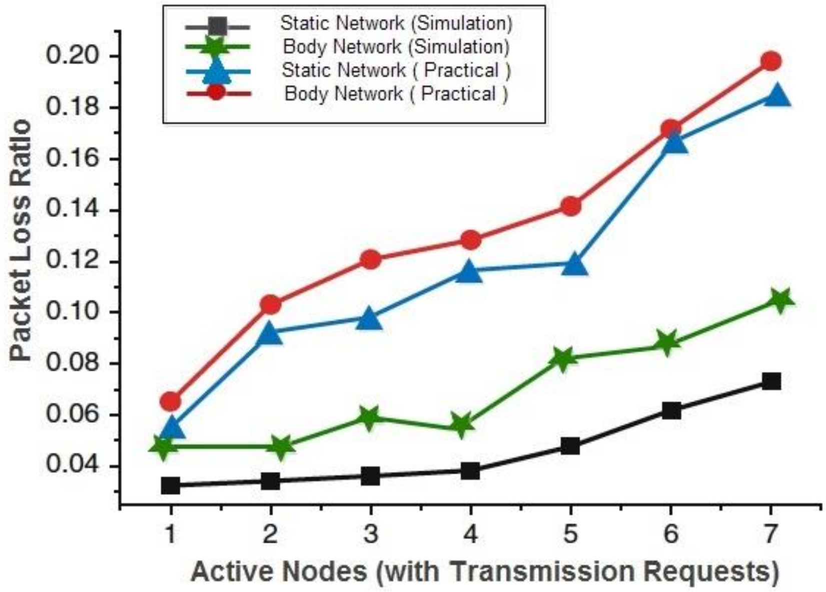

Fig.5.6. Packet Loss (Simulation vs. Practical).

In Figure 5.6, it is observed that the packet loss in a real hardware platform is slightly higher than the packet loss in simulation platform, this is obvious as hardware model has hidden channel conditions which impact the transmission. It is also observed that the packet loss for the static subnet is lower than the packet loss for the dynamic subnet. That means there human body has its (own) resistance for the data communication.

Average Event based Delay

Event based delay is a specific performance test, was executed by forcing an emergency trigger (e.g. pulse data stopped, or multiple sensors are interested in transmitting event data). For the simulation test, data feed was executing a loop for 30 seconds with sensed data “0”. During hardware implementation, a steel sheet was tagged between sensor and body for the same time (e.g. 30 seconds).

In this scenario at the application layer (MAS WBAN), delay time (when an event generated, and a time when BS got this information) was calculated. The test is executed in both ways, once when continue operating nodes were connected (parallel), and in the second one continue operating nodes were disconnected. This test has a direct link to MAC layer performance and as per the result, it is observed that once an event occurs, the packet delay increases. In practical (h/w) experiments, the delay is more in both network segments. That is realistic as the difference between the packet loss on simulation platform, and hardware platform is not huge (e.g. Delay for static networks b/w hardware and simulation results is just 0.011 s) similarly the delay for dynamic network segment b/w simulation and hardware is just 0.012 s).

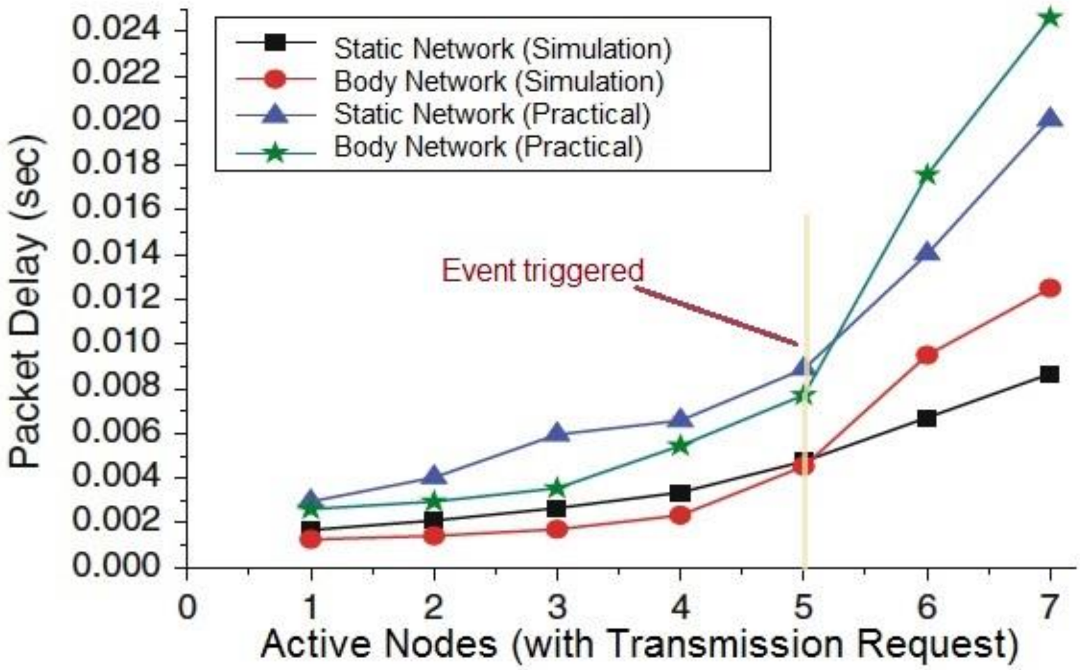

Fig.5.7. Event based Packet Delay (Simulation vs. Practical).

Figure 5.7 shows that the event based packet delay of sensor nodes in the static network is lower than that of the dynamic (body based) network, we can see a significant delay at 5, this is the point when 5^{th} nodes become active. Event based delay consists of the total time taken for queuing, medium access, inter-frame space, packet transmission, and event reception. Medium access delay consists of time taken for allocating a time slot in the next frame during random access of periodic sensor nodes and back-off time taken in case of an unsuccessful time slot allocation. In the hardware based implementation scenario only four periodic sensor nodes per CH have to contend for sending data, while, in a simulation scenario, all the periodic sensor nodes contend for a single shared medium. As the number of sensor nodes increases above a certain limit, the time delay that a sensor node is required to wait to send data through the shared medium will increase. Scenarios show that the allocated time increases considerably after total periodic sensor nodes increase above 5. It is also observed that contention in the links between the CH and BS the coordinator in hardware implementation scenario is much lower than the contention level in the links between sensor nodes and coordinator in the simulation scenario. From the results, it can be concluded that simulation platform has better performance though hardware results are less in performance but more realistic.

Throughput Analysis

Since priority is given for critical event data, throughput of continuous data should be kept at a high (periodic signals like humidity, light is comparatively less time critical.) Hence, it is reasonable to allocate a higher priority to continuous sensor nodes.

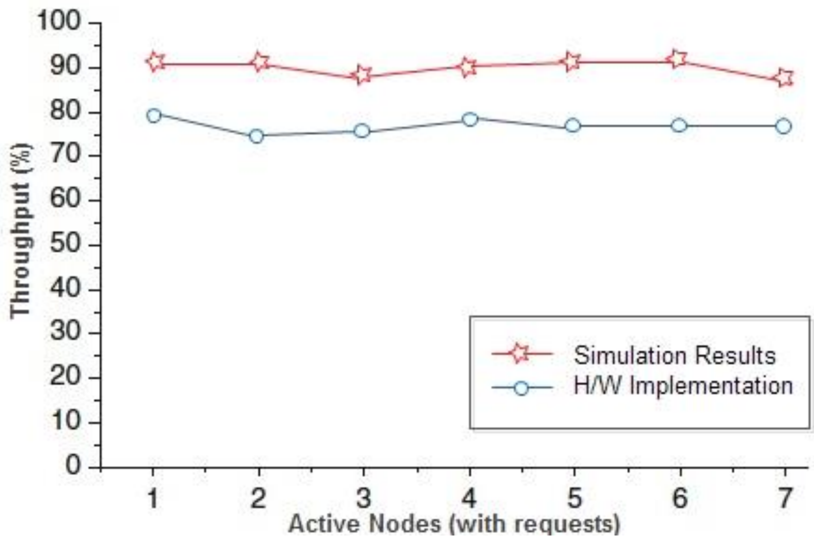

Fig.5.8. Throughput (Simulation vs. Practical).

For the throughput analysis instead of testing the individual throughput of each network segment, the overall throughput of the whole platform is calculated and compared. From Fig. 5.8, it can be seen that throughout the experiment percentage of simulation platform, for both static and dynamic networks is higher than the hardware based implementation. It is also observed that in the real network situation, as traffic increases throughput decreases. Though throughput of h/w implementation is less than the simulation implementation results, the important point is its consistency. During the experiment throughput performance remains around 75 %, even in the case of 7 active nodes. Throughout the experiments average throughput for h/w implementation is 77 %, whereas for the same simulation throughput is 88 %. That is very realistic and acceptable margin and proves the effectiveness of the proposed framework.

Energy Consumption

A framework with low power consumption will allow the battery powered sensor network to operate in an autonomous manner with less human intervention.

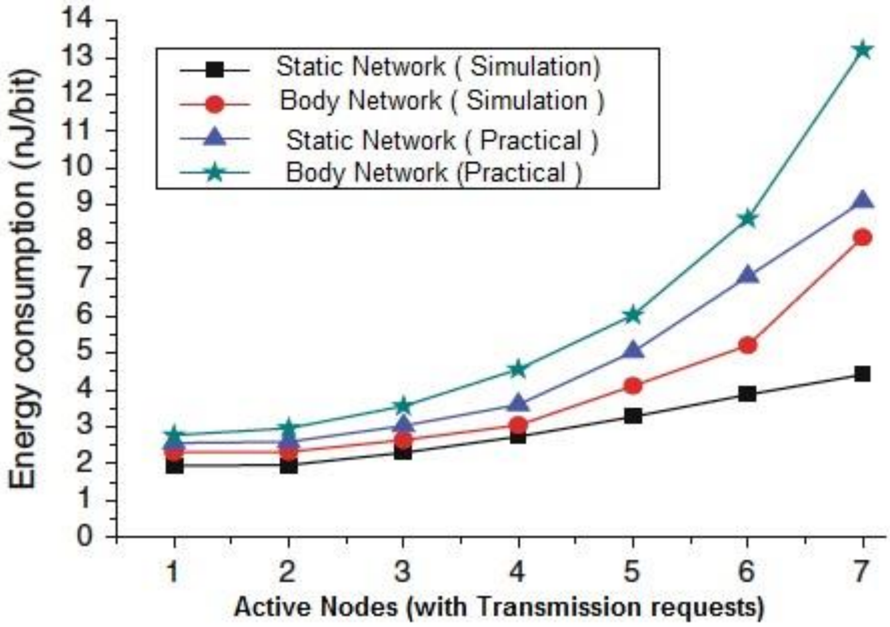

Fig.5.9. Energy Consumption (Simulation vs. Practical).

From Figure 5.9 it can be observed that the consumed energy at sensor nodes per useful bit is comparatively higher in hardware based implementation. Also includes the power consumption of retransmissions. By comparing the number of retransmissions for both platforms (simulation and hardware), it is observed that in simulation platform, it is less than that of hardware based implementation. Such outcomes are natural and acceptable as simulation platforms are usually not 100 % but close to reality. In the Simulation based scenarios, to achieve a given bit error rate (10^{-4}), the transmit power of the sensor node is kept at a minimum. Hence, the number of pulses that needs to be transmitted is comparatively lower than of hardware based scenarios. Since the channel characteristics of the receiver are relatively constant over short distances, the need for dynamically changing the number of pulses is lessened. Because of all these factors the sensor nodes in simulation-based scenario consume less power than sensor nodes of hardware based scenario.

RESULTS AND CONCLUSIONS

The Doctoral Thesis is focused on architecture design of ultra wideband impulse radio in wireless sensor network, for light and dense networks. The research results have been practically tested in real test bed under project "Smart Incubator".

The main findings of the Doctoral Thesis:

1) Existing MAC algorithms (U-MAC, Leach etc.) were re-stimulated under Impulse Radio and based on the outcome bottlenecks (energy, synchronization, scheduling) a new multi-phase MAC algorithm (Pilot assisted MAC) is designed. A transmission strategy PAT (Pilot assisted Transmission) was integrated with the MAC algorithm and its performance was compared with existing MACs by repeating simple to complex scenarios.
2) A Radio Layer architecture TRDH (Transmitted Reference Delay Hoped) was developed by combining Transmitted Reference and Delay hoped technique focusing on the doublet (PAT) method. For the multi-user capability, Voltera model was added to the Radio architecture. *BER* performance was compared with the existing market standards RAKE, and WAKE-Up by different scenarios.
3) A dynamic clustering technique was added to the architecture which formats clusters based on transmission range an aggregated Cost function is used for the efficient energy control. The use of such formation enhanced the capability of architecture and it can be used for dense network environment.
4) Implementation of adaption features was tested for the self-healing capability of the network for both light and dense network with over dozens different complex scenarios, where self-healing was tested for different complex situations (e.g. Network behavior in case of Cluster head and a node death). Network lifetime, Delivery ratio and Residual all major performance parameters were analyzed.
5) The performance of the PA-MAC framework is compared between hardware and simulation platforms. For detailed analysis number of key findings e.g. Energy consumption, packet delay, and Throughput is thoroughly examined between two. Further, to that, each platform's individual performance is also considered (e.g. static segment, dynamic network segment).

By relating the simulation results with the real hardware based results, it can be concluded that PA-MAC is an adoptable new approach for future wireless sensor networks. Results also proved that the UWB based PA-MAC architecture is as effective in a real bed as on simulation bed.

Future development directions:

- To broaden the implementation area by using the proposed architecture in Urban traffic Control Sensor network.
- To add the security mechanism in the architecture so it could be used for a critical security domain.

REFERENCES

[1] Fowler, M. Highsmith, J., The agile manifesto // Software Development. vol. 9, no.3 , 2001 pp. 28–35.

[2] Ayub, K., IR-UWB Radio Architecture for Wireless Sensors Network Based on Pilot Signal Assisted MAC // in 2014 6th International Conference on New Technologies, Mobility and Security (NTMS), 2014, Dubai, Mar. 2014, pp. 1–5.

[3] Ayub, K. Zagurskis, V., Pilot signal assisted Ultra Wideband medium access control algorithm for Wireless Sensor Networks // in 2013 21st Telecommunications Forum Telfor (TELFOR). Nov. 2013, pp. 184–187.

[4] Ayub, K. Zagurskis, V., Technology Implications of UWB on Wireless Sensor Network- A detailed Survey // International Journal of Communication Networks and , Information Security (IJCNIS), Volume 7, No.3. pp. 1–14.

[5] Zhao, D., Xi, L., Tang, X., Zhang, W., Qiao, Y., Zhang, X., Digital pilot aided carrier frequency offset estimation for coherent optical transmission systems. // Opt. Express volume. 23, no. 19. 2015 pp. 24–32.

[6] Mathews, V. . Sicuranza, G. ., Polynomial Signal Processing, Illustrate.. New York: John Wiley & Sons Ltd, 2000- 260p.

[7] Rousselot, J. Decotignie, J.D., An ultra-wideband impulse radio PHY layer model for network simulation // Simulation vol. 87, no. 1, Jul. 2010 pp. 82–112.

[8] Mohanty, R., Behera, H. S., Patwari, K., Dash, M., Prasanna, M. L., Priority Based Dynamic Round Robin (PBDRR) Algorithm with Intelligent Time Slice for Soft Real Time Systems // (IJACSA) International Journal of Advanced Computer Science and Applications, vol. 2, no. 2, 2011 pp. 46-50.

[9] Tao, L., Qing-Xin, Z., Luqiao, Z., An Improvement for LEACH Algorithm in Wireless Sensor Network // , in Industrial Electronics and Applications (ICIEA), 2010, pp. 1811–1814.

[10] Jurdak, R., Baldi, P., Lopes, C. V., U-MAC: A proactive and adaptive UWB medium access control protocol // Wirel. Commun. Mob. Comput. vol. 5, no. 5 2005 pp. 551–566.

[11] El Fawal, A., Le Boudec, J. Y., Merz, R., Radunovic, B., Widmer, J., Maggio, G. M., Trade-off analysis of PHY-Aware MAC in low-rate low-power UWB networks // IEEE Commun. Mag. vol. 43, no. 12 Dec. 2005 pp. 147–155.

[12] ZOU, D., GAO, L., LI, S., Volterra filter modeling of a nonlinear discrete-time system based on a ranked differential evolution algorithm // J. Zhejiang Univ. vol. 15, no. 8, 2014

pp. 687–696.

[13] Oppermann, I., Stoica, L., Rabbachin, A., Shelby, Z., Haapola, J., UWB wireless sensor networks: UWEN - A practical example // IEEE Commun. Mag. vol. 42, no. 12 2004. pp. 317-322.

[14] Li, F., Xiao, H., Yang, J., On channel estimation for RAKE receiver in a mobile multipath fading channel // , in Proceedings of ICASSP ’94. IEEE International Conference on Acoustics, Speech and Signal Processing, pp. 577–580.

[15] Ha, T. T., Theory and Design of Digital Communication Systems, no. 2010. Cambridge University Press, 2010-629p.

[16] Calhoun, G. M., Third Generation Wireless Systems, Volume 1, no. 2003. Artech House, 2003-473p.

[17] Latiff, N. M. A., Tsimenidis, C. C., Sharif, B. S., Kingdom, U., Energy-Aware Clustering for Wireless Sensor Networks Using Particle Swarm Optimization // 18th Annual IEEE Int. Sysmposium Pers. Indoor Mob. Radio Commun, 2007 pp. 5–9.

[18] Orcioni, S., Pirani, M., Turchetti, C., Advances in Lee-Schetzen method for Volterra filter identification // , in Multidimensional Systems and Signal Processing, no. 2005, pp. 265–284.

[19] Ayub, K. Zagurskis, V., Adoption features and approach for UWB Wireless Sensors Network based on Pilot Signal assisted MAC // International Journal of Communication Networks and , Information Security (IJCNIS), Volume 8, No.1. pp.20-46.

[20] Kaur, H. Seehra, P. A., Performance Evaluation of Energy Efficient Clustering Protocol for CH selection in Wireless // International Journal of Peer to Peer Networks (IJP2P) Vol.5, No.3, August 2014. pp. 1-13.

[21] Naruephiphat, W. Charnsripinyo, C., An Energy-aware Clustering Technique for Wireless Sensor Networks // pp. 189–211.

[22] W. Elmenreich, F. Dressler, V. Loreto, Self-Organizing Systems// 7th IFIP TC6 International Workshop, IWSOS 2013, Palma de Mallorca, Spain, May 9-10, 2013, Revised Selected Papers, Springer, 2014-191p.

[23] Dressler, F., A Study of Self-Organisation Mechanisms in Ad Hoc and Sensor Networks // Comput. Commun. vol. 31, no. 13 2008 pp. 3018–3029.

[24] Simulation Technologies in Networking and Communications: Selecting the Best Tool for the Test, vol. 6, no. 2014. CRC Press, 2014.

[25] Yuce, M. R., Redouté, J. M., Thotahewa, K. M., Keong, H. C., Development of low-power UWB body sensors // Int. Symp. Commun. Inf. Technol. 2012 pp. 143–148.

[26] Chase, R., UWB: Fostering Innovation Through Balanced Regulatory Framework, Engineering Technol. no. 2006-p37.

[27] Hoctor, R. Tomlinson, H., Delay-hopped transmitted-reference RF communications // IEEE Conf. Ultra Wideband Syst. Technol. (IEEE Cat. No.02EX580). 2002 pp. 265–270.

[28] Zhang, H. Z. H. Goeckel, D. L., Generalized transmitted-reference UWB systems // IEEE Conf. Ultra Wideband Syst. Technol. 2003. pp. 147-151.

[29] Abraha, S. T., Okonkwo, C. M., Tangdiongga, E., Koonen, a. M. J., Experimental demonstration of 2 Gbps IR-UWB transmission over 100m GI-POF using novel pulse generation technique // 36th Eur. Conf. Exhib. Opt. Commun. 2010 pp. 1–3.

[30] IEEE, Federal Communications Commission, Ultra-wideband (UWB) first report and order. internet: http://www.ieee802.org/15/pub/TG3a.html. [Accessed: 12-Jun-2015].

[31] Robert, B., Labview 7 Express, Prentice Hall, Vol 2009. pp. 133–145.

[32] Yusuf Khan, J., Yuce, M. R., Bulger, G., Harding, B., Wireless body area network (WBAN) design techniques and performance evaluation // Journal of Medical Systems vol. 36, no. 3, 2012. pp. 1441–1457.